

Absence of *N*-Acetylaspartate in the Human Brain: Impact on Neurospectroscopy?

Ernst Martin, MD,¹ Andrea Capone, MD,²
Jacques Schneider, MD,¹ Juergen Hennig, PhD,³ and
Thorsten Thiel, PhD^{1,3}

***N*-acetylaspartate (NAA) contributes to the most prominent signal in proton magnetic resonance spectroscopy (¹H-MRS) of the adult human brain. We report the absence of NAA in the brain of a 3-year-old child with neurodevelopmental retardation and moderately delayed myelination. Since normal concentration of NAA in body fluids is hardly detectable, ¹H-MRS is a noninvasive technique for identifying neurometabolic diseases with absent NAA. This report puts NAA as a neuronal marker to question.**

Ann Neurol 2001;49:518–521

Proton magnetic resonance spectroscopy (¹H-MRS) of the human brain provides noninvasive quantitative metabolic information from amino acids (*N*-acetylaspartate [NAA], alanine, and glutamate), from amines (glutamine, choline, and creatine), from sugars (myo-inositol and glucose), and from compounds involved in high-energy metabolism (creatine and lactate). During recent years, pediatric neurospectroscopy has shed new light on metabolic mechanisms of normal brain development^{1,2} and on metabolic diseases of the infant brain.^{3–6} Today, ¹H-MRS is a noninvasive clinical examination with an American Medical Association billing code on U.S. Food and Drug Administration–approved equipment.

NAA contributes to the most prominent signal in ¹H-MRS of the human brain beyond the age of 3 years. NAA is almost exclusively present in the central nervous system, where it is predominantly located in pyramidal neurons, dendrites, and axons;⁷ in oligodendrocyte type 2 astrocyte progenitor cells; and in immature⁸ and even mature oligodendrocytes.⁹ Being specific to neural tissue, NAA is said to signify viable brain cells and denote neuronal density reflecting various cellular compositions, which are in agreement with histological findings.¹⁰ NAA is implicated in many processes of the nervous system, such as the regulation of neuronal protein synthesis, brain lipid production, and the metabolism of aspartate and

N-acetyl-aspartyl-glutamate (NAAG).¹¹ Moreover, it was found to play a role in protecting neurons from osmotic stress.¹² NAAG has been observed in early maturing cells, predominantly in neocortical pyramidal cells, and in specific neuronal populations of the basal ganglia and thalamus thought to use gamma-aminobutyric acid (GABA) as a neurotransmitter.¹³

Here, we are reporting for the first time the absence of NAA and NAAG in the entire brain of a 3-year-old boy with neurodevelopmental retardation and moderately delayed myelination.

Case Report

This 3-year-old boy was born at term as the second child of a 20-year-old woman in an Eastern European country. He was brought to a foster home, from which he was adopted. At birth, weight and height were 2780 gm and 54 cm, respectively. The head circumference taken at the age of 6 weeks was 37.5 cm. A neonatal blood screening for phenylketonuria and hypothyroidism, a urinalysis for amino acids and mucopolysaccharides, a cranial ultrasound study, a serologic examination for toxoplasmosis, and an ophthalmological examination were performed before adoption. Results of these examinations were reported to be normal. No more information concerning the family history or the pregnancy was provided by the authorities.

A developmental delay, with slowing of milestones, soon became apparent, although there was no concern about vision or hearing. Somatic growth for height and weight followed along the twenty-fifth percentile, whereas the head circumference progressively fell below the third percentile by the age of 19 months. At this age, a developmental quotient of 0.5 necessitated supportive educational measures.

At the age of 3 years, he was able to sit unaided and to walk a few steps broad based. No neurologic deficits were noted. He vocalized sounds but expressed no meaningful words. He was not dysmorphic and could understand simple commands. The electroencephalogram (EEG) was unremarkable. Results of the following biochemical investigations were normal: urine screening for amino acids, organic acids, and oligo- and mucopolysaccharides; serum creatine kinase and lactate determinations; HIV serologic studies; and karyotypic studies. The cerebrospinal fluid (CSF) was also unremarkable for protein, glucose, cell count, biogenic amines, folate, and pterines. CSF was examined by high-resolution magnetic resonance *in vitro* spectroscopy.

Methods and Results

Magnetic resonance imaging (MRI) and ¹H-MRS studies were carried out on a 2 T whole body scanner (Bruker-Medical S200A, Fällanden, Switzerland) on two occasions: at the age of 2 years and 3 months and at 3 years and 6 months. On the first occasion, except for patchy T2-

From ¹Neuroradiology and Magnetic Resonance, Department of Diagnostic Imaging, ²the Department of Neurology, University Children's Hospital Zurich, Zurich, Switzerland; and ³the Section of Medical Physics, University Hospital Freiburg, Freiburg, Germany.

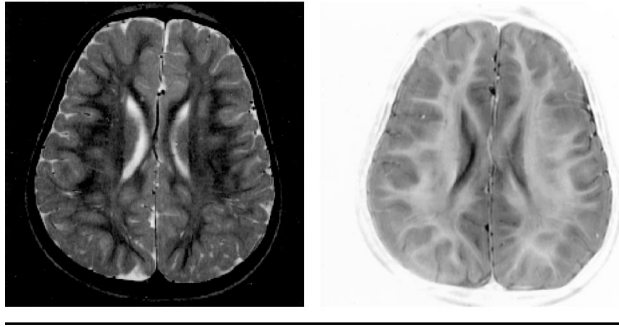


Fig 1. Axial T2-weighted image (left) shows mild patchy hyperintensities in the frontal and parietal (peritrigonal) deep white matter. These changes are hypointense to the normal white matter on the inversion recovery image (right) and are interpreted as moderately delayed myelination.

hyperintensities in the centrum semiovale and the peritrigonal white matter of both hemispheres, most probably representing areas of moderately delayed myelination, the MRI appeared surprisingly unremarkable. No signs of cerebral or cerebellar atrophy were present. At follow-up, the patchy white matter changes were still existent despite a clear progression in myelination on MRI (Fig 1).

Quantitative fully relaxed (repetition time [TR] 6000 msec) single-voxel (PRESS) spectra were acquired from the parietal white matter, the occipital and frontal gray matter, the basal ganglia, and the cerebellum. Short echo times (echo time [TE] 30 msec) were chosen for absolute metabolite quantification using the LCModel algorithm¹⁴ and the unsuppressed water resonance as an internal reference. Long-echo time spectra (TE 270 msec) were also obtained to separate signals from NAA at 2.02 ppm from overlapping resonances of glutamine, glutamate, and GABA. Sixty-four scans were averaged using voxel sizes of 6 ml. All spectra obtained on both occasions demonstrate absence of NAA in all examined brain regions (Fig 2b–e). This becomes even more obvious in spectra with long echo times. No signal at 2.02 ppm is detectable, and overlapping signals from glutamine, glutamate, and GABA have vanished due to j-coupling effects (Fig 2e).

The concentration of the other detectable metabolites are within age-appropriate normal limits (Table). No accumulation of the NAA precursor aspartate and insignificant amounts of lactate are found. At 3.75 ppm, an unusual resonance is

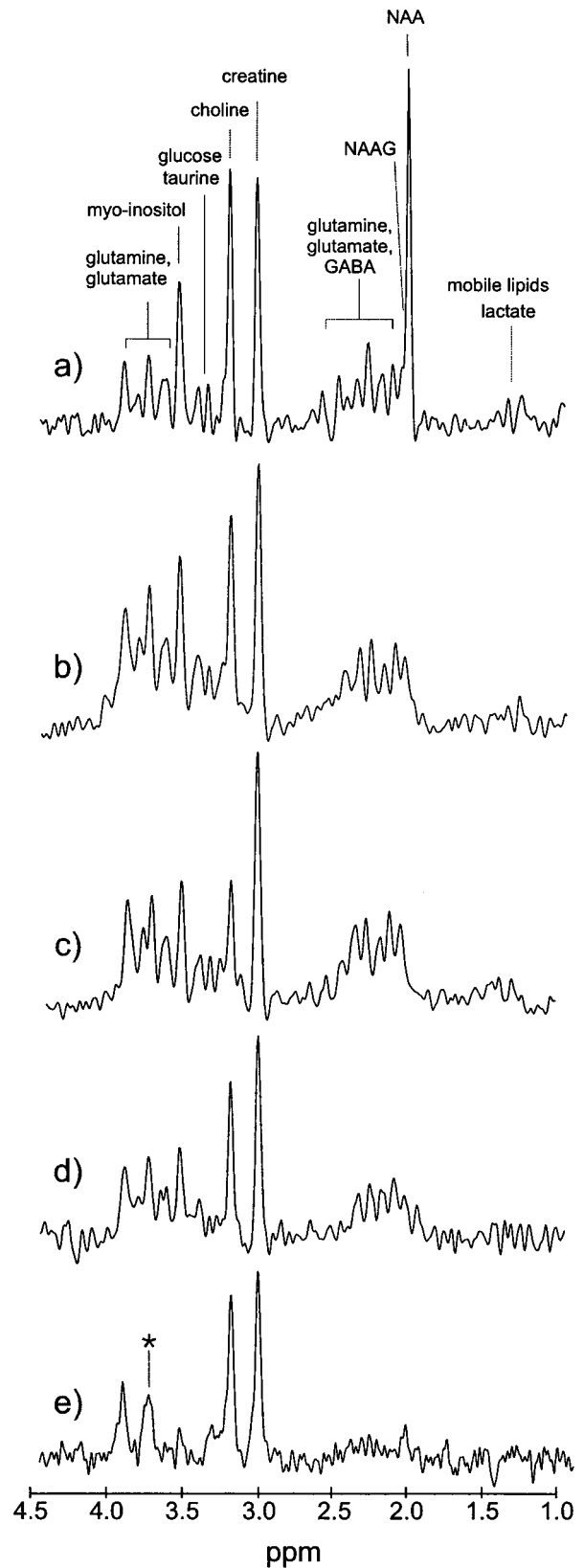


Fig 2. (a) An age-matched normal proton spectrum from the occipital gray matter with the prominent N-acetylaspartate (NAA) resonance at 2.02 ppm. (b–e) Complete absence of NAA in the spectra from different brain regions of the patient at age 3 years and 6 months. (b) Occipital gray matter. (c) Parieto-occipital white matter. (d) Basal ganglia. The absence of NAA becomes even more obvious in the long-echo time spectrum. (e) Parieto-occipital white matter at TE = 270 msec. At 3.75 ppm the unusual resonance is indicated.

Table. Metabolite Concentrations (mmol/kg Wet Weight) from Different Regions of the Boy's Brain

Brain Metabolites	Occipital Gray Matter	Parietal White Matter	Cerebellum	Basal Ganglia	Basal Ganglia Control Values
NAA + NAAG	0.95 ± 0.39	0.79 ± 0.29	1.37 ± 0.76	0.00 ± 0.00	10.99 ± 0.54
Myoinositol	3.44 ± 0.86	3.82 ± 0.38	6.55 ± 0.91	1.92 ± 0.96	3.67 ± 0.71
Lactate	1.13 ± 0.28	0.83 ± 0.27	0.67 ± 0.79	0.84 ± 0.52	0.70 ± 0.37
Creatine	6.68 ± 0.53	6.18 ± 0.37	9.69 ± 0.87	7.19 ± 0.65	7.42 ± 0.44
Glutamate	4.84 ± 0.58	3.45 ± 0.34	2.97 ± 1.01	4.54 ± 0.54	4.71 ± 0.56
Glutamine	3.08 ± 0.92	3.24 ± 0.64	4.20 ± 1.76	1.45 ± 1.10	3.21 ± 0.54
Choline	0.74 ± 0.09	1.11 ± 5.14	1.64 ± 0.18	1.36 ± 0.15	1.35 ± 0.11
Aspartate	0.46 ± 0.31	0.00 ± 0.00	0.00 ± 0.00	0.00 ± 0.00	0.00 ± 0.00

NAA = *N*-acetylaspartate; NAAG = *N*-acetyl-aspartyl-glutamate.

Age-matched normal control values from the basal ganglia (last column) are shown for comparison.

present in all spectra (see Fig 2). This resonance was not observed by *in vitro* CSF high-resolution spectroscopy.

Discussion

The pool of NAA constitutes NAA and NAAG, with variation of NAA concentrations in different brain regions. Biochemical and spectroscopic studies have demonstrated low concentrations of NAA in preterm infants, which increase during human brain maturation in parallel with the progress of myelination to reach almost adult levels by the age of 3 years.² While the neuronal density decreases during late gestation and early postnatal life, increasing NAA concentrations might reflect the process of differentiation and maturation of dendrites, axons, and synapses together with neuronal soma. Although there are still uncertainties about the precise function of NAA,¹⁵ most publications in this field are based on the assumption that NAA is a neuronal marker. Moreover, the cerebral concentration of NAA has been correlated with mental development,¹⁶ and low concentration has been proposed to signify reduced numbers of neurons in pediatric patients with mental retardation and developmental anomalies.¹⁷ Low NAA levels were said to indicate neurodegenerative disease,¹⁸ cognitive impairment,¹⁹ and adverse neurodevelopmental outcome in neonates with hypoxic-ischemic encephalopathy.²⁰

To our knowledge, no living subject, human or animal, has yet been reported with undetectable concentrations of NAA and NAAG in the brain. In line with the present theory on the role of NAA, the absence of NAA in all brain regions would imply substantial disintegration and extensive loss of viable neuroaxonal tissue. We have no indication that this is the case in this child from MRI, nor would it be compatible with his sensorimotor and even cognitive performance. We therefore propose that the concentration of NAA, as determined by *in vivo* ¹H-MRS, can no longer be taken as an indicator of viable neuronal tissue and that the functional role of NAA in the brain must be reevaluated in order to correctly interpret neurospectroscopic results in a clinical setting.

Considering the metabolism of NAA, we hypothesize a block of the biosynthesis of NAA at the level of acetyl-CoA-L-aspartate-*N*-acetyltransferase (ANAT), which converts L-aspartate to NAA, because we found no signal from degradation products in the spectra (i.e., acetate, L-aspartate, or NAAG). A block of ANAT would cause an accumulation of NAA precursors (e.g., L-aspartate or acetyl-CoA). Both precursors are involved in many metabolic pathways and therefore are not expected to accumulate. We might speculate that the resonance at 3.75 ppm, which is normally not present in brain spectra of healthy individuals, signifies an as yet unidentified metabolic precursor. The neuroimaging findings are consistent with moderately delayed myelination, since the normal concentrations of choline and myoinositol indicate neither gliosis nor active demyelination, as seen in leukoencephalopathies. To date, there are only two other reports of instances in which neurospectroscopy has provided key evidence of a new neurometabolic disease.^{4,6}

Our results from MRI and ¹H-MRS and from the as yet normal biochemical and genetic findings let us conclude that this boy may suffer from a new neurometabolic disease. Moreover, they emphasize the crucial role of *in vivo* ¹H-MRS in detecting neurometabolic diseases with low levels or an absence of NAA in the brain, since the concentration of NAA in body fluids is almost undetectably low.

This study was supported by a grant of the Swiss National Research Foundation, No. 32-52647.97.

We thank Professor Eugen Boltshauser and Professor Beat Steinmann from the University Children's Hospital Zurich for fruitful discussions and Professor Ron A. Wevers, University Medical Centre Nijmegen, for *in vitro* spectroscopy of CSF.

References

1. Kreis R, Ernst T, Ross B. Development of the human brain: *In vivo* quantification of metabolite and water content with proton magnetic resonance spectroscopy. *Magn Reson Med* 1993;30:424-437

2. Pouwels PJ, Brockmann K, Kruse B, et al. Regional age dependence of human brain metabolites from infancy to adulthood as detected by quantitative localized proton MRS. *Pediatr Res* 1999;46:474–485
3. Bruhn H, Kruse B, Korenke G, et al. Proton NMR spectroscopy of cerebral metabolic alterations in infantile peroxisomal disorders. *J Comput Assist Tomogr* 1992;16:335–344
4. Stoekler S, Holzbach U, Hanefeld F, et al. Creatine deficiency in the brain: a new, treatable inborn error of metabolism. *Pediatr Res* 1994;36:409–413
5. Tzika AA, Ball WS, Vigneron DB, et al. Clinical proton MR spectroscopy of neurodegenerative disease in childhood. *Am J Neuroradiol* 1993;14:1267–1281
6. Van der Knaap MS, Wevers RA, Struys EA, et al. Leukoencephalopathy associated with a disturbance in the metabolism of polyols. *Ann Neurol* 1999;46:925–928
7. Simmons ML, Frondoza CG, Coyle JT. Immunocytochemical localization of *N*-acetyl-aspartate with monoclonal antibodies. *Neuroscience* 1991;45:37–45
8. Urenjak J, Williams SR, Gadian DG, Noble M. Specific expression of *N*-acetyl-aspartate in neurons, oligodendrocyte-type-2 astrocyte progenitors, and immature oligodendrocytes in vitro. *J Neurochem* 1992;59:55–61
9. Bhakoo KK, Pearce D. In vitro expression of *N*-acetyl-aspartate by oligodendrocytes: implications for proton magnetic resonance spectroscopy signal in vivo. *J Neurochem* 2000;74:254–262
10. Ebisu T, Rooney WD, Graham SH, et al. *N*-Acetyl-aspartate as an in vivo marker of neuronal viability in kainate-induced status epilepticus: H-1 magnetic resonance spectroscopic imaging. *J Cereb Blood Flow Metab* 1994;14:373–382
11. Birken DL, Oldendorf WH. *N*-acetyl-L-aspartic acid: a literature review of a compound prominent in 1H-NMR spectroscopic studies of brain. *Neurosci Biobehav Rev* 1989;13:23–31
12. Taylor DL, Davies SE, Obrenovitch TP, et al. Investigation into the role of *N*-acetyl-aspartate in cerebral osmoregulation. *J Neurochem* 1995;65:275–281
13. Moffett JR, Namboodiri MA. Differential distribution of *N*-acetyl-aspartyl-glutamate and *N*-acetyl-aspartate immunoreactivities in rat forebrain. *J Neurocytol* 1995;24:409–433
14. Provencher S. Estimation of metabolite concentrations from localized in vivo NMR spectra. *Magn Reson Med* 1993;30:672–679
15. Clark JB. *N*-acetyl-aspartate: a marker for neuronal loss or mitochondrial dysfunction. *Dev Neurosci* 1998;20(4–5):271–276
16. Jung RE, Brooks WM, Yeo RA, et al. Biochemical markers of intelligence: a proton MR spectroscopy study of normal human brain. *Proc R Soc Lond B Biol Sci* 1999;266:1375–1379
17. Hashimoto T, Tayama M, Miyazaki M, et al. Reduced *N*-acetyl-aspartate in the brain observed on in vivo proton magnetic resonance spectroscopy in patients with mental retardation. *Pediatr Neurol* 1995;13:205–208
18. Hanefeld F, Kruse B, Bruhn H, Frahm J. In vivo proton magnetic resonance spectroscopy of the brain in a patient with L-2-hydroxyglutaric acidemia. *Pediatr Res* 1994;35:614–616
19. Meyerhoff DJ, Mackay S, Bachman L, et al. Reduced brain *N*-acetyl-aspartate suggests neuronal loss in cognitively impaired human-immunodeficiency-virus-seropositive individuals: in vivo H-1 magnetic resonance spectroscopic imaging. *Neurology* 1993;43:509–515
20. Groenendaal F, Veenhoven RH, van der Grond J, et al. Cerebral lactate and *N*-acetyl-aspartate/choline ratios in asphyxiated full-term neonates demonstrated in vivo using proton magnetic resonance spectroscopy. *Pediatr Res* 1994;35:148–151

A Novel TRK A (*NTRK1*) Mutation Associated with Hereditary Sensory and Autonomic Neuropathy Type V

Henry Houlden, MRCP,¹ R. H. M. King, PhD,² A. Hashemi-Nejad, FRCS (Orth),³ N. W. Wood, MD,¹ C. J. Mathias, MD,⁴ Mary Reilly, MD,¹ and P. K. Thomas, DSc¹

A boy with recurrent pyrexial episodes from early life sustained a painless ankle injury and was found to have a calcaneus fracture and, later, neuropathic joint degeneration of the tarsus. Examination revealed distal loss of pain and temperature sensation and widespread anhidrosis. Sural nerve biopsy demonstrated severe reduction in small-caliber myelinated fiber density but only modest reduction in unmyelinated axons, the pattern of type V hereditary sensory and autonomic neuropathy (HSAN V). DNA analysis showed that he was homozygous for a mutation in the *NTRK1*/high-affinity nerve growth factor (*TrkA*) gene, his parents being heterozygous. Mutations in this gene are known to be responsible for HSAN IV (congenital insensitivity to pain with anhidrosis). The two disorders are therefore likely to be allelic.

Ann Neurol 2001;49:521–525

Swanson¹ reported two brothers with congenital insensitivity to pain, anhidrosis, and mild mental retardation. Postmortem examination was performed on one of them at the age of 12 years,² and it revealed an absence of Lissauer's tracts and reduced numbers of small dorsal root ganglion cells. Goebel et al³ later reported a normal total density of myelinated nerve fibers but a possible reduction in those of smaller size. Unmyelinated axons were virtually absent. This autosomal recessive disorder has been termed congenital insensitivity to pain with anhidrosis (CIPA),¹ or type IV hereditary sensory and autonomic neuropathy (HSAN IV).⁴ Mutations in the gene for the high-affinity nerve

From the ¹ University Department of Clinical Neurology, Institute of Neurology; ² Department of Clinical Neurosciences, Royal Free and University College Medical School; ³ Royal National Orthopaedic Hospital; and ⁴ Autonomic Research Unit, Institute of Neurology, London, United Kingdom.

Received Sep 25, 2000, and in revised form Dec 14. Accepted for publication Dec 16, 2000.

Address correspondence to Dr Thomas, University Department of Clinical Neurology, Institute of Neurology, Queen Square, London WC1N 3BG, United Kingdom. E-mail: pkt.hotline@virgin.net

growth factor receptor, TrkA (NTRKA), have been found in a small number of families.⁵⁻⁷

A phenotypically similar disorder has been categorized as type V HSAN.⁴ The original singleton cases showed a congenital loss of pain sensation, impaired sweating, preserved muscle strength, and retained tendon reflexes.^{4,8} Donaghy et al⁹ described a similar autosomal recessive disorder. In all these cases, nerve biopsy showed a selective loss of small myelinated fibers. Unmyelinated axon density was only slightly reduced. The main difference between HSAN IV and HSAN V is, therefore, the pattern of nerve fiber loss and the greater severity of the anhidrosis in the former. The present report suggests that HSAN IV and V are not distinct disorders but different manifestations of mutations in the *NTRK1* gene.

Case Report

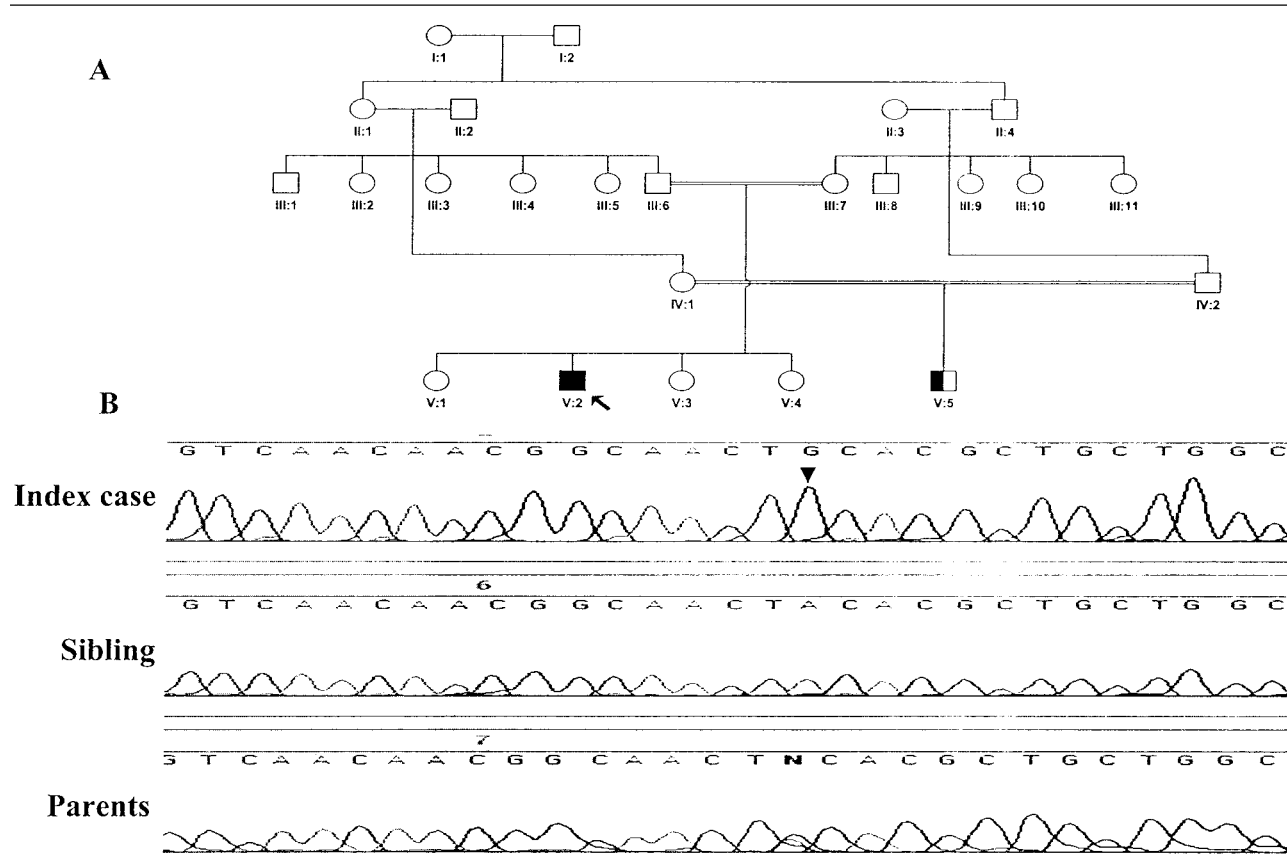
A Pakistani boy aged 9 years was born to healthy but consanguinous parents (Fig 1A). The pregnancy and birth were normal, as were early developmental milestones. During early childhood in Pakistan, he had recurrent episodes of pyrexia, up to 40°C, during hot

weather. His father noticed that during these his skin was dry and he failed to sweat. After moving to the United Kingdom when aged 6 years, his pyrexial episodes became less frequent. They were treated by putting him under a cold shower. Bladder and bowel function was normal. When he was younger, he had had recurrent syncopal attacks.

In 1998, the patient fell, injuring his right ankle. No pain was experienced until 2 to 3 days later. His ankle became swollen. A fracture of the calcaneus was diagnosed and treated by a plaster cast. Further radiological investigations because of persistent ankle swelling showed damage to the neck of the talus and a sclerotic lesion in the cuboid. Magnetic resonance imaging demonstrated synovial thickening and joint effusions. Tuberculous infection was excluded.

Neurologically, cranial nerve function, motor function in the limbs, and tendon reflexes were normal. Plantar responses were flexor. Light touch and joint position sense was normal. Pinprick and temperature sense was lost distally in the limbs. Deep pain sensibility in his feet was absent bilaterally. His peripheral nerves were not thickened.

Fig 1. (A) Pedigree of the family. Squares = male; circles = female; filled symbol = affected individual; half-filled symbol = affected by history; arrow = index case. (B) *NTRK1* exon 8 sequence in the index case and family. The arrowhead indicates the missense mutation of an A to a G at position 1076, changing a tyrosine to a cysteine at codon 359. The index case is homozygous GG, his unaffected parents and one unaffected sibling are heterozygous AG, and another unaffected sibling is homozygous AA.



In the family history (see Fig 1A) a male cousin, also born to consanguinous parents, is known to have anhidrosis.

Results

Nerve Conduction Studies

Peroneal motor nerve conduction was normal (conduction velocity 46 m/sec, distal motor latency 3.5 msec, F wave latency 39 msec), but compound muscle action potential amplitude was reduced (1.4 mV, knee and ankle stimulation). Sural and superficial peroneal sensory action potential amplitudes were slightly reduced (8 μ V, 6 μ V) with normal conduction velocities (41 m/sec, 44 m/sec).

Autonomic Function Tests

There was no evidence of orthostatic hypotension, and there was normal sinus arrhythmia. Pressor test responses were mildly impaired (simple spelling, cutaneous cold challenge, and hyperventilation). No galvanic skin responses were detectable in the feet on inspiratory gasps. Plasma adrenaline and dopamine levels were normal when resting or on tilting. Plasma noradrenaline levels were slightly reduced (139 pmg/ml; 168 pmg/ml tilted; normal 200–500 pmg/ml).

Nerve Biopsy

Sural nerve fascicular biopsy was undertaken and the specimen processed by standard techniques.¹⁰ Myelinated fiber density was 7,669/mm² (normal value for same age 10,979/mm²). There was a relative deficiency of small myelinated fibers (Fig 2,3). No actively degenerating fibers, signs of regenerative activity, or hypertrophic changes were detected. Myelin thickness was normal, as assessed by g ratio (axon diameter/total fiber diameter) distributions. On electron microscopic examination, unmyelinated axon density was slightly reduced, at 26,920/mm², compared with an age-matched control value of 35,700/mm².¹¹ No abnormal axonal or Schwann cell inclusions were seen. The blood vessels and connective tissues appeared normal.

Genetic Analysis

DNA was extracted from blood samples obtained from affected and unaffected family members. The 17 exons and flanking intronic regions of the *NTRK1* gene were amplified by polymerase chain reaction (PCR).^{7,13} PCR products were purified (Qiaquick purification kit Qiagen, Hilden, Germany) and sequenced on an ABI377 automated sequencer (BigDye Terminator cycle sequencing kit, Perkin-Elmer, Foster City, USA).

A novel missense mutation was identified in exon 8 at codon 359 causing a tyrosine-to-cysteine amino acid change. This was homozygous in the index case and heterozygous in both parents and one unaffected

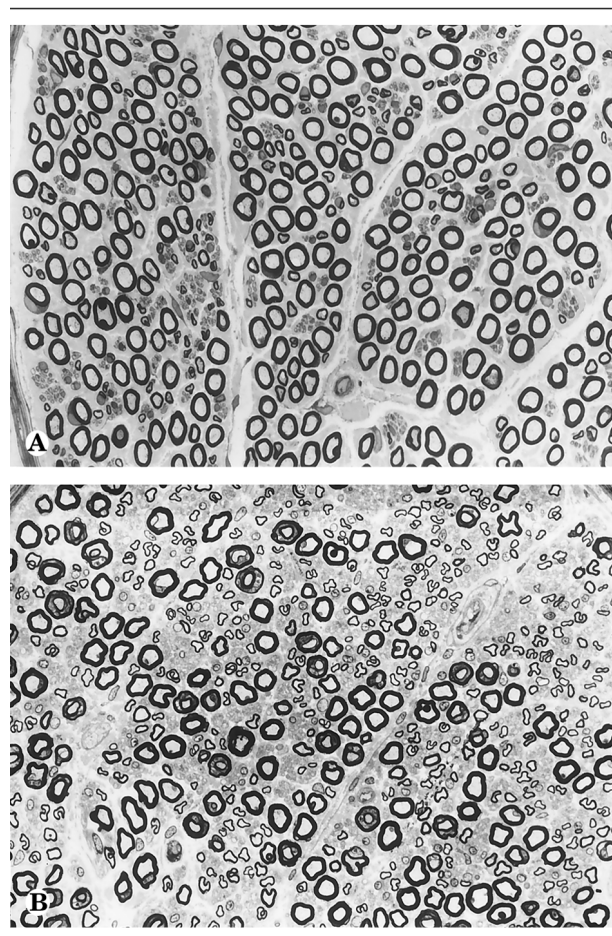


Fig 2. Portions of transverse sections of (A) a sural nerve biopsy specimen from the patient and (B) a postmortem specimen from Case 13 of Jacobs and Love¹¹ showing lack of small myelinated fibers in A. Thionin and acridine orange, $\times 480$.

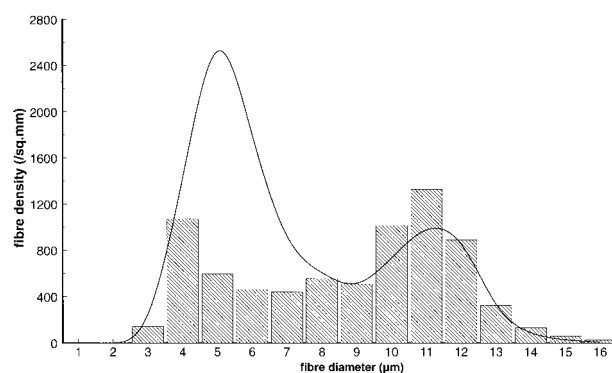


Fig 3. Myelinated fiber size distribution for the patient (histogram) and Case 13 from Jacobs and Love¹¹ (continuous line) showing depletion of small myelinated fibers in the patient.

daughter; another unaffected daughter was homozygous for the normal base (see Fig 1B). This mutation was not found in 30 Pakistani and 50 Caucasian control subjects by sequencing. Two further novel base

changes were identified in exon 15, both creating an amino acid change: histidine 598 tyrosine and glycine 607 valine. These two changes were in disequilibrium with each other, consistent with close genetic proximity. Both base changes were present in Pakistani (3 heterozygotes in 30 individuals) and Caucasian (1 homozygote and 13 heterozygotes in 80 individuals) control subjects. Two other polymorphisms were present in the family and control subjects, both silent changes, exon 14 CAA–CAG 1656 and exon 15 GCC–GCT base 1869. Polymorphism segregation was consistent with recessive inheritance.

Polymorphic markers located close to the *NTRK1* gene were analyzed in the family. These markers were D1S2878, D1S484, D1S196, D1S2726, D1S252, D1S218, and D1S498. Each marker was amplified, diluted, and pooled according to protocol (Perkin-Elmer ABI Linkage Mapping Set version 2.0) and run on an AB1377 automated sequencer and analyzed using ABI Genescan and Genotyper software. This showed genetic linkage to the *NTRK1* gene in an autosomal recessive fashion with homozygosity in markers across the *NTRK1* region.

Discussion

The index case in the present family showed a combination of widespread congenital anhidrosis and distally accentuated loss of pain and temperature sensibility. He had minor abnormalities of vasomotor function without orthostatic hypotension. Recurrent syncopal attacks had occurred in early childhood, usually provoked by injury or emotional factors. It is of interest that syncope was a feature in one of the original cases of CIPA reported by Swanson.¹ As was pointed out by Dyck et al,⁴ the designation CIPA is a misnomer. The neurological changes are manifestations of a peripheral neuropathy, as evidenced by the distal distribution of the sensory loss and sudomotor dysfunction.

Sural nerve biopsy showed a reduction in small myelinated fiber density, with preservation of density for larger-caliber fibers and relative preservation of unmyelinated axons. This is the pattern described for HSAN V, as distinct from the virtual absence of unmyelinated axons in HSAN IV.⁴ As already stated, HSAN IV is due to mutations in the *NTRK1* gene; functional studies have shown that these result in inactivation of the *NTRK1*/nerve growth factor receptor.¹³

The exon 8 tyrosine 359 cysteine *NTRK1* mutation is pathogenic and likely to cause partial loss of gene function and a less severe deficiency of unmyelinated axons but a greater effect on small myelinated fibers. Alternatively, *NTRK1* expression could be modulated by the presence of rare polymorphisms in the gene. Other reported mutations in the *NTRK1* gene lead to a phenotype of HSAN IV. The majority of these mutations cause aberrant splicing or truncation and usually result

in a more significant effect on *NTRK1* mRNA than does the missense mutation reported.^{7,13,14} This codon has been mutated to a stop codon in a Japanese patient with a more severe clinical phenotype and sural nerve biopsy findings consistent with HSAN IV.¹⁵ It will be important to analyze the *NTRK1* gene in other families with HSAN V to define the spectrum of the mutations, the mechanism of action, and the way in which particular mutations lead to different pathological phenotypes.

An unresolved question, alluded to by Donaghy et al.⁹ and Dyck,¹⁶ is how to explain the severe distal loss of pain sensibility in face of the relatively modest loss of small myelinated fibers in HSAN IV and a similar mild reduction in unmyelinated axons in HSAN V. Landrieu et al.¹⁷ reported a mother and daughter with “congenital indifference to pain” in whom other forms of sensation and autonomic function were preserved, as were sensory action potentials. Nerve biopsy findings were normal, with normal numbers and size distributions of myelinated and unmyelinated axons. An agnosia for pain is unlikely because the mother had experienced pain from dental treatment. An abnormality of transmitter function or of central pain pathways would thus have to be considered, and such an abnormality may thus be an additional deficit in HSAN IV and V.

This study was supported by the Wellcome Trust (H.H., P.K.T., and R.H.M.K.).

We thank Dr Jean Jacobs for access to the control nerve specimen, Michelle Nourallah for performing the morphometric studies, and John Muddle for writing the programs and analyzing the results.

References

1. Swanson AG. Congenital insensitivity to pain: a unique syndrome in two male siblings. *Arch Neurol* 1963;8:299–306.
2. Swanson AG, Buchan GG, Alvord EC Jr. Autonomic changes in congenital insensitivity to pain: absence of small primary sensory neurons in ganglia, roots and Lissauer's tract. *Arch Neurol* 1965;12:12–18.
3. Goebel HH, Veit S, Dyck PJ. Confirmation of virtual unmyelinated fiber absence in hereditary sensory neuropathy type IV. *J Neuropathol Exp Neurol* 1980;39:670–675.
4. Dyck PJ, Mellinger JF, Reagan TJ, et al. Not “indifference to pain” but varieties of hereditary sensory and autonomic neuropathy. *Brain* 1983;106:373–390.
5. Indo Y, Tsuruta M, Hayashida Y, et al. Mutations in the TRKA/NGF receptor gene in patients with congenital insensitivity to pain with anhidrosis. *Nat Genet* 1996;13:485–488.
6. Yotsumoto S, Setoyama M, Hozumi H, et al. A novel point mutation affecting the tyrosine kinase domain of the TRKA gene in a family with congenital insensitivity to pain with anhidrosis. *J Invest Dermatol* 1999;112:810–814.
7. Mardy S, Miura Y, Endo F, et al. Congenital insensitivity to pain with anhidrosis: novel mutations in the TRKA (*NTRK1*) gene encoding a high-affinity receptor for nerve growth factor. *Am J Hum Genet* 1999;64:1570–1579.
8. Low PA, Burke WJ, McLeod JG. Congenital sensory neuropathy with selective loss of small myelinated fibers. *Ann Neurol* 1978;3:179–182.

9. Donaghy M, Hakin RN, Bamford JM, et al. Hereditary sensory neuropathy with neurotrophic keratitis: description of an autosomal recessive disorder with a selective reduction of small myelinated nerve fibres and a discussion of the classification of the hereditary sensory neuropathies. *Brain* 1987;110:563–583.
10. Tournev I, King RHM, Workman J, et al. Peripheral nerve abnormalities in the congenital cataracts facial dysmorphism neuropathy (CCFDN) syndrome. *Acta Neuropathol* 1999;98:165–170.
11. Jacobs JM, Love S. Qualitative and quantitative morphology of human sural nerve at different ages. *Brain* 1985;108:897–924.
12. Roa BB, Warner LE, Garcia CA, et al. Myelin protein zero (MPZ) gene mutations in nonduplication type 1 Charcot-Marie-Tooth disease. *Hum Mutat* 1996;7:36–45.
13. Greco A, Villa R, Fusetti L, et al. The Gly571Arg mutation, associated with the autonomic and sensory disorder congenital insensitivity to pain with anhidrosis, causes the inactivation of the NTRK1/nerve growth factor receptor. *J Cell Physiol* 2000;182:127–133.
14. Miura Y, Mardy S, Awaya Y, et al. Mutation and polymorphism analysis of the *TRKA* (*NTRK1*) gene encoding a high-affinity receptor for nerve growth factor in congenital insensitivity to pain with anhidrosis (CIPA) families. *Hum Genet* 2000;106:116–124.
15. Iwanaga R, Matsuishi T, Ohnishi A, et al. Serial magnetic resonance images in a patient with congenital sensory neuropathy with anhidrosis and complications resembling heat stroke. *J Neurol Sci* 1996;142:79–84.
16. Dyck PJ. Neuronal atrophy and degeneration predominantly affecting peripheral sensory and autonomic neurons. In: Dyck PJ, Thomas PK, Griffin JW, et al, eds. *Peripheral neuropathy*. Philadelphia: W.B. Saunders, 1993;1065–1093.
17. Landrieu P, Said G, Allaire C. Dominantly transmitted congenital indifference to pain. *Ann Neurol* 1990;27:574–578.

Subthalamic Infusion of an NMDA Antagonist Prevents Basal Ganglia Metabolic Changes and Nigral Degeneration in a Rodent Model of Parkinson's Disease

Fabio Blandini, MD,¹ Giuseppe Nappi, MD,^{1,2}
and J. Timothy Greenamyre, MD, PhD³

Using permanent cannulas connected to subcutaneous pumps, we infused selective glutamate antagonists into the subthalamic nucleus of rats. Pumps were implanted immediately after the intrastriatal injection of 6-hydroxydopamine and delivered micro-quantities of the *N*-methyl-D-aspartate antagonist MK-801 or the α -amino-3-hydroxy-5-methylisoxazole antagonist NBQX for 4 weeks. Subthalamic infusion of MK-801, but not of NBQX, prevented the basal ganglia metabolic changes and motor abnormalities caused by nigrostriatal lesion. Animals treated with MK-801 also exhibited marked reduction of nigral cell loss. We conclude that pharmacological modulation of subthalamic activity may have both symptomatic and neuroprotective effects in Parkinson's disease.

Ann Neurol 2001;49:525–529

In Parkinson's disease (PD), nigrostriatal degeneration triggers a cascade of changes in basal ganglia circuitry, which leads to overactivity of the subthalamic nucleus (STN) and its projection nuclei, medial globus pallidus (MGP) and substantia nigra pars reticulata (SNr).¹ Recent evidence suggests that STN overactivity may also contribute to the progression of PD. In addition to its main targets, the STN also sends excitatory projections to the substantia nigra pars compacta (SNc).^{2,3} Therefore, subthalamic disinhibition might cause glutamatergic overstimulation of residual SNc neurons. A number of factors, including oxidative stress and mitochondrial defects, might reduce the ability of nigral neurons to

From the ¹Laboratory of Functional Neurochemistry, Neurological Institute C. Mondino, Pavia, Italy; ²Institute of Nervous and Mental Diseases, La Sapienza University, Rome, Italy; and ³Departments of Neurology and Pharmacology, Emory University, Atlanta, GA.

Received Jul 7, 2000. Accepted for publication Dec 18, 2000.

Address correspondence to Dr Blandini, Laboratory of Functional Neurochemistry, Neurological Institute C. Mondino, Via Palestro, 3 27100 Pavia, Italy. E-mail: blandini@tin.it

cope with a potentially harmful agent, such as glutamate.¹ This enhanced glutamatergic input to the SNC may therefore aggravate—via a mechanism known as “indirect excitotoxicity”⁴—the progression of the disease, leading to a vicious cycle in which STN overactivity and nigral damage support each other.⁵ Indeed, in rats, ablation of the STN counteracts the SNc degeneration caused by intrastriatal administration of 6-hydroxydopamine (6-OHDA)⁶ or 3-nitropropionic acid.⁷

The aim of this study was to investigate whether chronic reduction of STN glutamatergic transmission interferes with the development of the nigrostriatal lesion and the resulting basal ganglia functional changes caused by 6-OHDA. For this purpose, we infused selective antagonists of either the *N*-methyl-D-aspartate (NMDA) or the α -amino-3-hydroxy-5-methylisoxazole propionic acid (AMPA) glutamate receptor subtype into the STN of rats immediately after the striatal injection of 6-OHDA. As opposed to the direct injection of 6-OHDA into the SNc, which causes massive and rapid cell loss, intrastriatal injection of 6-OHDA causes a partial SNc lesion that evolves gradually. This technique is therefore recommended when evaluating neuroprotective strategies for experimental PD.⁸

Material and Methods

Male Sprague-Dawley rats (250–300 gm) were used. All animal care and use was in accordance with National Institutes of Health guidelines and was approved by the Institutional Animal Care and Use Committee (IACUC) of Emory University. The NMDA blocker MK-801 and the AMPA blocker NBQX, in its water-soluble form (1,2,3,4-tetrahydroxy-6-nitro-2,3-dioxo-benzo quinoxaline-7-sulfonamide disodium), were purchased from RBI (Natick, MA). Drugs were dissolved in saline solution.

Surgical Procedures

Animals were anesthetized with ketamine (75 mg/kg) and xylazine (10 mg/kg) and placed in a stereotactic apparatus. They received a 3.5- μ l injection of 6-OHDA (2.5 μ g/ μ l plus 0.2 μ g/ μ l ascorbate) into the right striatum (1 mm an-

terior, 3 mm lateral with respect to bregma, and 4.5 mm ventral with respect to dura) at a rate of 0.5 μ l/min. Immediately after, a 28-gauge infusion cannula was lowered into the ipsilateral STN (3.7 mm posterior, 2.4 mm lateral with respect to bregma, and 7.9 mm ventral with respect to dura). The cannula base was secured to the skull with dental cement and anchor screws and connected to a subcutaneous mini-osmotic pump placed on the back of the animal (Alzet Brain Infusion kit, Alza, Palo Alto, CA).

Drugs

Pumps were loaded with 10 μ M MK-801, 50 μ M NBQX, or saline solution (control animals) and delivered into the STN at a rate of 4.2 nl/min for 4 weeks. Given the absence of previous studies with similar experimental conditions, we chose concentrations of MK-801 and NBQX known to be highly effective in *in vitro* conditions.^{9,10}

Behavioral Testing

At the third week, animals were tested with systemic amphetamine (3 mg/kg, intraperitoneally) to evaluate the behavioral effect (turning behavior) of the evolving nigrostriatal lesion. Rotational response to the drug was expressed as the number of full (360-degree) turns per minute.

Histochemistry

At the end of the fourth week, animals were killed by decapitation. Brains were rapidly removed, frozen on dry ice, and stored at -70°C . Frozen coronal sections (25 μ m) containing striatum, globus pallidus (GP, the rodent structure homologous to the lateral globus pallidus), entopeduncular nucleus (EP, the rodent structure homologous to the MGP), STN, SNr, and SNc were cut and mounted on slides. Sections were stained for activity of cytochrome oxidase (CO), a functional marker of neuronal activation,^{11,12} using a metal-enhanced histochemical technique described recently.¹³ The cell loss in the SNc was evaluated by means of Nissl staining, which was also used to verify the correct location of striatal injections and subthalamic cannulas.

Image Analysis

A densitometric comparison of CO activity in the two hemispheres was carried out using a computerized video-based

Table. Cytochrome Oxidase Activity in the Striatum, Globus Pallidus (GP), Entopeduncular Nucleus (EP), Subthalamic Nucleus (STN), and Substantia Nigra Pars Reticulata (SNr) of Rats with Unilateral Nigrostriatal Lesion and Ipsilateral Intrasubthalamic Infusion of Saline Solution (Control Animals), MK-801, or NBQX

	Striatum		GP		EP		STN		SNr	
	Intact	Lesioned	Intact	Lesioned	Intact	Lesioned	Intact	Lesioned	Intact	Lesioned
Control animals (n = 9)	413 \pm 22	455 ^a \pm 21	97 \pm 9	133 ^a \pm 13	82 \pm 6	116 ^b \pm 11	526 \pm 46	587 \pm 45	221 \pm 31	283 ^a \pm 35
MK-801 (n = 7)	420 \pm 23	419 \pm 24	135 \pm 17	152 \pm 16	94 \pm 19	111 \pm 21	647 \pm 62	497 ^a \pm 48	260 \pm 36	253 \pm 36
NBQX (n = 6)	423 \pm 19	455 ^c \pm 19	128 \pm 9	168 ^b \pm 13	89 \pm 15	124 ^b \pm 9	544 \pm 64	593 \pm 55	210 \pm 19	291 ^b \pm 21

^a*p* < 0.005 vs intact side (Student's *t* test for paired data).

^b*p* < 0.01 vs intact side (Student's *t* test for paired data).

^c*p* < 0.05 vs intact side (Student's *t* test for paired data).

Values (mean \pm SEM) are expressed as optical density units ($\times 1000$).

image analysis system (Imaging Research, St. Catharines, Ontario, Canada). The same system was used to count the Nissl-positive cells in the SNc. In both cases, the average value of at least four adjacent sections was considered as representative of each area.

Statistics

Comparisons between groups were made using one-way analysis of variance (ANOVA) followed by a Fisher's post-hoc test. Side-to-side comparisons within the same group were made by Student's *t* test for paired data. Minimum level of statistical significance was set at $p < 0.05$.

Results

Only animals in which both the striatal 6-OHDA injection and subthalamic cannula were correctly located were considered for the data analysis.

CO Activity

Control animals showed significant increases in CO staining in the striatum, GP, EP, and SNr ipsilaterally to the nigrostriatal lesion (Table). CO activity was also increased in the ipsilateral STN, although not significantly. Animals that received subthalamic infusion of MK-801 showed a significant reduction of CO activity in the STN and no significant asymmetries in any of the other nuclei evaluated (Fig 1). Like control animals, the animals that received subthalamic NBQX showed significant increases in CO activity in the striatum, GP, EP, and SNr ipsilaterally to the nigrostriatal lesion as well as a slight, nonsignificant increase in the ipsilateral STN.

Nigral Damage

Control animals showed discrete cell loss (30%) in the right SNc compared with the left SNc. Animals treated with subthalamic MK-801 but not with NBQX showed a significant reduction of the nigral cell loss with respect to control animals (Fig 2A).

Rotational Behavior

Control animals showed consistent rotational behavior in response to systemic amphetamine (Fig 2B). The response was significantly reduced in the animals that received subthalamic MK-801 but not NBQX.

Discussion

Glutamate antagonists have repeatedly proven beneficial in animal models of PD.¹⁴ In this study, we continuously infused selective ionotropic glutamate antagonists into the STN with the aim of investigating whether chronic blockade of glutamatergic transmission at the level of the STN could influence the SNc damage and resulting functional changes caused by 6-OHDA.

In control animals, the intrastriatal injection of 6-OHDA caused discrete SNc cell loss. CO activity was significantly increased in the striatum, GP, EP, and SNr ipsilaterally to the lesion and nonsignificantly in the STN. Subthalamic infusion of MK-801 but not NBQX decreased CO activity in the nucleus, prevented the metabolic changes in the other basal ganglia nuclei, and reduced the degree of the SNc cell loss. The rotational response to amphetamine observed in

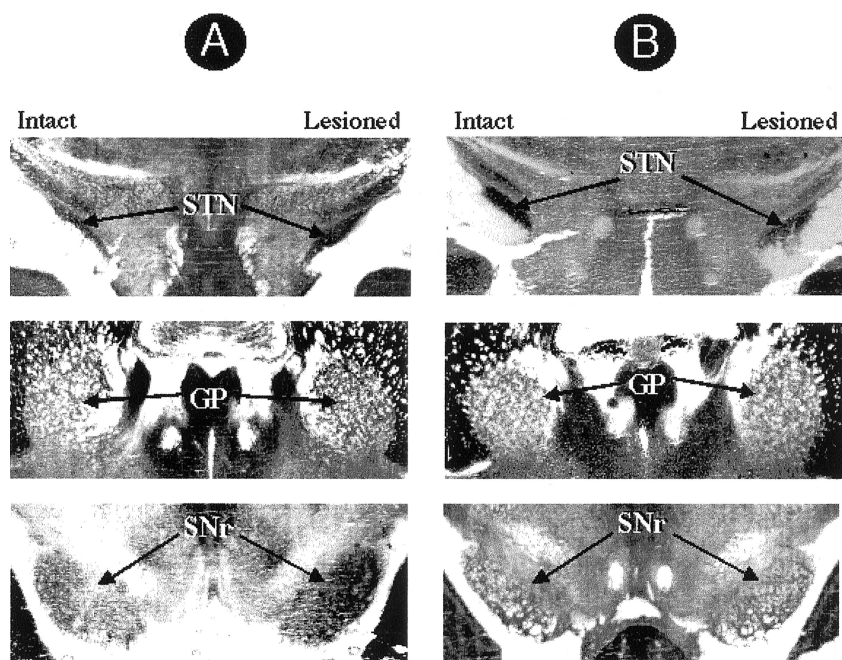


Fig 1. Brain coronal sections stained for cytochrome oxidase activity. The sections, which contain subthalamic nucleus (STN), globus pallidus (GP), and substantia nigra pars reticulata (SNr), were obtained from a control animal (A) and from an animal that, in addition to the intrastriatal injection of 6-hydroxydopamine, received a 4-week intrasubthalamic infusion of MK-801. (B) Note how, in the control specimen, the staining is more intense in the STN, GP, and SNr on the lesioned side. Conversely, the animal treated with MK-801 shows a clear reduction of cytochrome oxidase activity in the STN (where the drug was infused) and no metabolic asymmetries in GP and SNr.

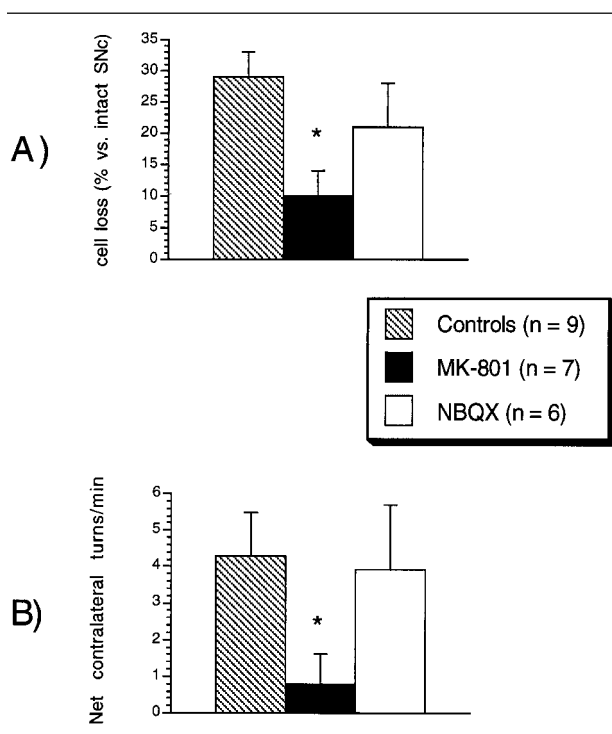


Fig 2. (A) Nigral damage. Bars represent the mean (\pm SEM) reduction in the number of Nissl-positive neurons of the lesioned substantia nigra pars compacta (SNc) compared with the intact SNc. Animals that received intrasubthalamic infusion of MK-801 showed a significant reduction of the nigral damage (ANOVA, $F = 3.7$, $p < 0.05$; Fisher's post-hoc test (asterisk), $p < 0.05$ vs control animals). (B) Rotational behavior. Animals treated with MK-801 showed significant reduction in the rotational response to amphetamine compared with control animals (ANOVA, $F = 3.55$, $p < 0.05$; Fisher's post-hoc test (asterisk), $p < 0.05$ vs control animals).

control animals was also abolished in animals treated with MK-801.

Our metabolic data confirm that nigrostriatal lesion, even of limited degree, leads to overactivity of basal ganglia output nuclei.¹ Such overactivity is sustained by the STN, since the reduction of STN activity caused by MK-801 abolished these changes.

The origin of STN overactivity is currently disputed. According to classical models of basal ganglia organization, the activity of GP—which normally inhibits STN—should decrease following nigrostriatal lesion. This would cause STN disinhibition.¹⁵ In fact, we found that GP metabolic activity increased, rather than decreased, after nigrostriatal lesion. This confirms previous observations and suggests that STN overactivity has different sources.^{16,17} For example, given the reciprocal connections between STN and SNc,^{3,18} degeneration of SNc might affect the STN directly. In addition, enhanced excitatory inputs originating from both the brainstem and the thalamus reach the STN in rats bearing a nigrostriatal lesion.¹⁹

The striatum is not typically considered a target of STN projections, although a subthalamo-striatal pathway has been described.² It is interesting to note that the metabolic changes found in the striatum of both control animals and animals treated with NBQX were similar to those observed in the typical STN projection nuclei. Moreover, the intrasubthalamic infusion of MK-801 prevented the striatal metabolic changes. These findings confirm a previous observation²⁰ and suggest that modifications in STN activity can affect the striatum directly.

The fact that reducing STN activity through local infusion of MK-801 protected SNc neurons confirms that the STN plays a role in the progression of the nigral damage. Thus, once nigrostriatal degeneration begins (irrespective of cause), STN overactivity ensues, and glutamatergic stimulation of SNc neurons contributes to subsequent cell loss. It is interesting that no symptomatic or protective effects were seen when the AMPA receptor blocker NBQX was used, which points to a more important role of NMDA receptors in mediating the functional responses of the STN.

In conclusion, chronic blockade of NMDA receptor-mediated transmission in the STN had both symptomatic and neuroprotective effects in a rodent model of PD. Pharmacological manipulation of the STN, through selective drugs capable of modulating glutamatergic transmission, may therefore represent a valuable tool for the treatment of PD.

This study was supported by United States Public Health Service grant NS33779 (J.T.G.).

We thank Dr Ranjita Betarbet, Dr Roberto Fancellu, and Monica Garcia-Osuna for their assistance.

References

- Blandini F, Nappi G, Tassorelli C, Martignoni E. Functional changes of the basal ganglia circuitry in Parkinson's disease. *Progr Neurobiol* 2000;62:63–88.
- Kita H, Kitai ST. Efferent projections of the subthalamic nucleus in the rat: light and electron microscopic analysis with the PHA-L method. *J Comp Neurol* 1987;260:435–452.
- Smith Y, Charara A, Parent A. Synaptic innervation of mid-brain dopaminergic neurons by glutamate-enriched terminals in the squirrel monkey. *J Comp Neurol* 1996;364:231–253.
- Albin RL, Greenamyre JT. Alternative excitotoxic hypotheses. *Neurology* 1992;42:733–738.
- Rodriguez MC, Obeso A, Olanow W. Subthalamic nucleus-mediated excitotoxicity in Parkinson's disease: a target for neuroprotection. *Ann Neurol* 1998;44:S175–S188.
- Piallat B, Benazzouz A, Benabid AL. Subthalamic nucleus lesion in rats prevents dopaminergic nigral neuron degeneration after striatal 6-OHDA injection: behavioural and immunohistochemical studies. *Eur J Neurosci* 1996;8:1408–1414.
- Nakao N, Ekin N, Nakai K, Itakura T. Ablation of the subthalamic nucleus supports the survival of nigral dopaminergic neurons after nigrostriatal lesions induced by the mitochondrial toxin 3-nitropropionic acid. *Ann Neurol* 1999;45:640–651.
- Sauer H, Oertel WH. Progressive degeneration of nigrostriatal

- dopamine neurons following intrastriatal terminal lesions with 6-hydroxydopamine: a combined retrograde tracing and immunocytochemical study in the rat. *Neuroscience* 1994;59:401–415.
9. Bon CLM, Paulsen O, Greenfield SA. Association between the low threshold calcium spike and activation of NMDA receptors in guinea-pig substantia nigra pars compacta neurons. *Eur J Neurosci* 1998;10:2009–2015.
 10. Li S, Stys PK. Mechanisms of ionotropic glutamate receptor-mediated excitotoxicity in isolated spinal cord white matter. *J Neurosci* 2000;20:1190–1198.
 11. Wong-Riley MTT. Cytochrome oxidase: an endogenous metabolic marker for neuronal activity. *Trends Neurosci* 1989;12:94–101.
 12. Blandini F, Garcia-Osuna M, Greenamyre JT. Subthalamic ablation reverses changes in basal ganglia oxidative metabolism and motor response to apomorphine induced by nigrostriatal lesion in rats. *Eur J Neurosci* 1997;9:1407–1413.
 13. Divac I, Mojsilovic-Petrovic J, Lopez-Figueroa MO, et al. Improved contrast in histochemical detection of cytochrome oxidase: metallic ions protocol. *Neurosci Methods* 1995;56:105–113.
 14. Blandini F, Porter RHP, Greenamyre JT. Glutamate and Parkinson's disease. *Mol Neurobiol* 1996;12:1–17.
 15. Albin RL, Young AB, Penney JB. The functional anatomy of basal ganglia disorders. *Trends Neurosci* 1989;12:366–375.
 16. Vila M, Levy R, Herrero MT, et al. Metabolic activity of the basal ganglia in parkinsonian syndromes in human and non-human primates: a cytochrome oxidase histochemistry study. *Neuroscience* 1996;71:903–912.
 17. Hassani OK, Mouroux M, Feger J. Increased subthalamic neuronal activity after nigral dopaminergic lesion independent of disinhibition via the globus pallidus. *Neuroscience* 1996;72:105–115.
 18. Hassani OK, Feger J, Yelnik J, Francois C. Evidence for a dopaminergic innervation of the subthalamic nucleus in the rat. *Brain Res* 1997;749:88–94.
 19. Orioux G, Francois C, Feger J, et al. Metabolic activity of excitatory parafascicular and pedunculopontine inputs to the subthalamic nucleus in a rat model of Parkinson's disease. *Neuroscience* 2000;97:79–88.
 20. Blandini F, Greenamyre JT. Effect of subthalamic nucleus lesion on mitochondrial enzyme activity in rat basal ganglia. *Brain Res* 1995;669:59–66.

Germline Mutations in the *CCM1* Gene, Encoding Krit1, Cause Cerebral Cavernous Malformations

Miguel Lucas, MD¹, Alzenira F. Costa, PhD,¹
Mariano Montori, MD,² Francisca Solano, BS,¹
María D. Zayas, PhD,¹ and Guillermo Izquierdo, MD,³

Mutations in the Krit1 gene have been recently discovered as the cause of hereditary cerebral cavernous angioma. We sought the possibility that de novo, noninherited mutations of Krit1 also cause cavernous angioma. A patient with two cerebral malformations carries a heterozygous deletion of two base pairs (741delTC) in exon VI of the Krit1 gene. The deletion initiates a frameshift mutation that, 23 amino acids downstream, encodes a TAA stop triplet replacing a CAT triplet of histidine at exon VII (H271X). Magnetic resonance images of the parents were normal, neither parent carries the 741delTC mutation, and both bear the wild-type sequence of exon VI. These findings document a de novo germline mutation in Krit1 gene that causes cerebral cavernous malformations.

Ann Neurol 2001;49:529–532

Krit1 is an ankyrin repeat-containing protein that interacts with Krev-1/rap1a,¹ a protein described as a member of the Ras family of GTPases with probable tumor-suppressing activity in the cell. Truncating mutations in *CCM1*, the gene encoding Krit1 protein, cause hereditary cavernous angiomas,^{2,3} and a great variety of mutations have been described.^{2–4}

Familial forms of cerebral cavernous angiomas are manifested as multiple lesions and sporadic forms as a unique lesion, suggesting a “Knudson's double-loss mechanism,” that evoke hereditary and sporadic forms of tumorigenesis caused by tumor-suppressor genes.⁵ Although it is generally believed that some percentage of the patients with cavernous malformation represents new mutations, to our knowledge, de novo mutations causing cavernous angioma have not been previously

From the ¹Servicio de Biología Molecular, Hospital Universitario Virgen Macarena, Seville, Spain; ²Servicio de Neurología Hospital Miguel Servet, Zaragoza, Spain; and ³Servicio de Neurología, Hospital Universitario Virgen Macarena, Seville, Spain.

Received Aug 15, 2000, and in revised form Jan 3, 2001. Accepted for publication Jan 3, 2001.

Address correspondence to Dr Lucas, Servicio de Biología Molecular, Hospital Universitario Virgen Macarena, Avenida Dr Fedriani s/n, 41009 Seville, Spain. E-mail: lucas@cica.es

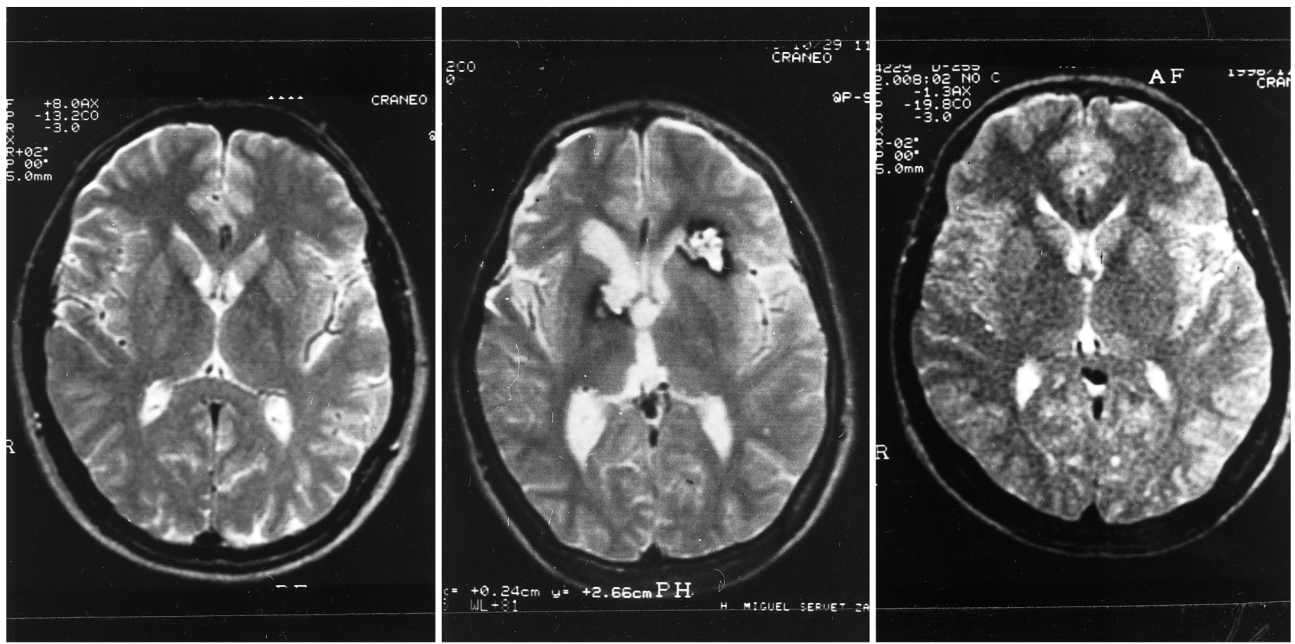


Fig 1. Magnetic resonance images (MRIs) of the patient and the parents. The screening of the whole brain by T2-weighted MRIs showed two cavernomas in the patient (middle), in contrast to the normal images of father (left) and mother (right). We did not find other malformations in the screening of the whole brains of the parents or the sister.

reported. We discovered a very illustrative single-strand conformation polymorphism (SSCP) in exon VI of the index patient of an a priori familial form. The absence of cavernous malformations in the parents and their normal SSCP patterns suggested a case of noninherited cavernous angioma, and therefore we sought a possible mutation of the *Krit1* gene. This possibility seems interesting in relation to the abovementioned pathogenic mechanism.

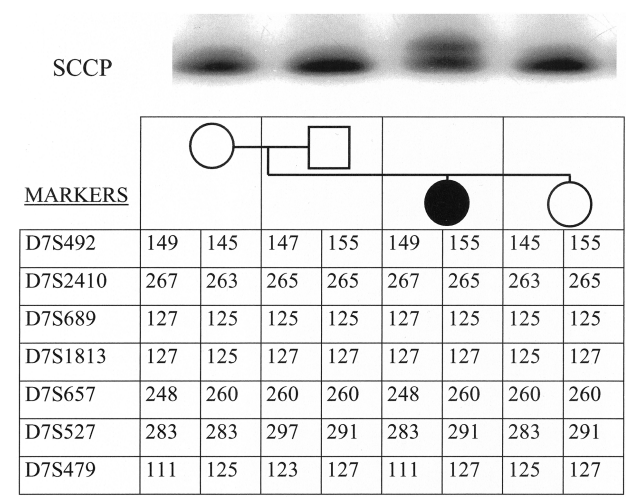
Patients and Methods

The main clinical characteristic of the proband consisted of headaches, whereas the parents and sister were almost symptoms free, except for the mother, who complained about headaches. Two cavernomas were discovered through T2-weighted magnetic resonance imaging (MRI) studies of the patient. MRI results were normal for the patient's parents and healthy sister.

CCM1 haplotypes of individuals of the CV36 family were analyzed with the protocols and primers as previously described.⁶ The polymorphic microsatellite markers spanning the *CCM1* interval were the following: D7S492, D7S2410, D7S1813, D7S689, D7S657, D7S527, and D7S479. A fragment of *Krit1* gene containing exon VI was amplified by polymerase chain reaction (PCR) techniques with primers forward (5'TTGTTAGATTGTGATGTA) and reverse (5'AACATAATAAACTTTC), as described recently.⁷ The nomenclature of cDNA refers to the work of Serebriiski et al,¹ although part of the *Krit1* gene was missed in this report, and additional exons have been identified very recently.⁸

Genomic DNA was initially screened by analysis of SSCP. PCR fragments were separated by electrophoresis in 10%

Fig 2. (Top) Single-strand conformation polymorphism (SSCP) of exon VI of *Krit1* gene of the Spanish family CVE36. Aliquots of DNA were amplified in the polymerase chain reaction (PCR) mixture containing [α^{32} P]-dCTP. Other reagents are described in Patients and Methods. The products of the PCR encompassing the exon VI were run under nondenaturing conditions in 10% acrylamide containing 10% glycerol for 16 hours at 20°C in a 20-by-30 cm gel. Bands were revealed after 48-hour exposure to x-ray films. The lower part of the figure shows the haplotypes of the critical region of *CCM1* in individuals of CV36 family. The corresponding markers are given in the first column. Note that both the affected and the healthy sibling inherited the same chromosome from the father and a different chromosome from the mother. Square = male; circle = female.



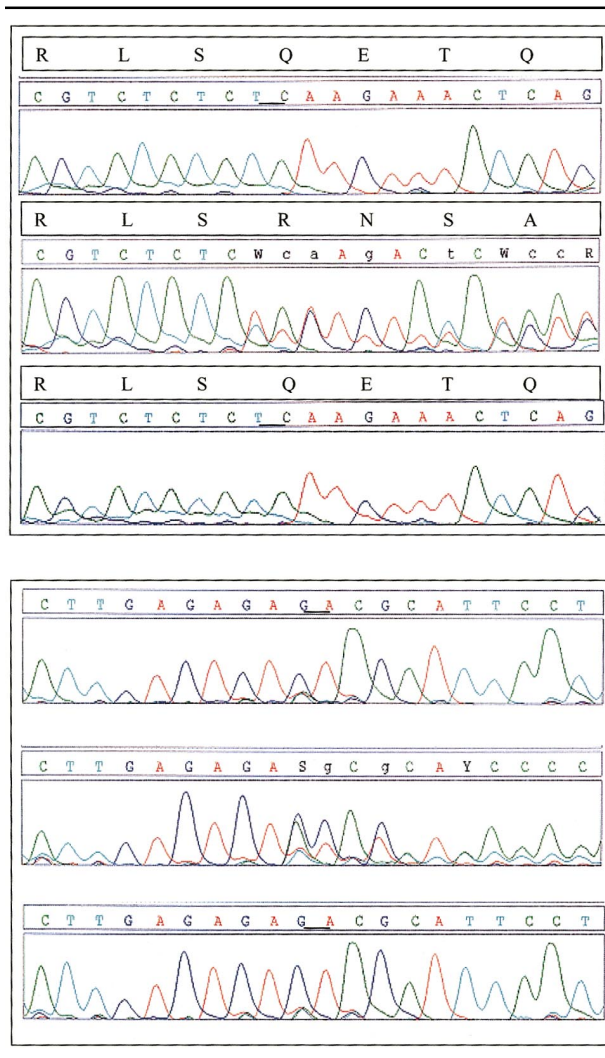


Fig 3. Comparison of the mutated and wild-type sequences of the sense (upper panel) and antisense (lower panel) strands surrounding the TC/AG deletion. The exon VI of genomic DNA of the father (upper traces), proband (middle traces), and mother (lower traces) were amplified by polymerase chain reaction techniques. The sequences of the products were determined with the 5'-IRD800-labeled forward (sense) and reverse (antisense) primers (see Patients and Methods) in an LI-COR 4000 autosequencer. The TC/GA pair (underlined in the wild-type chromosome) deletion displaces the sequences of the mutated strand. The amino acid sequences of the mutated and wild-type chromosomes are given above the nucleotide sequence of the sense strands. Ambiguities for mutated alleles are as follows: W, A or T; R, A or G; S, C or G; Y, C or T. Small letters indicate questionable base.

acrylamide in the absence and in the presence of 10% glycerol as described.²

DNA sequencing of exon VI was carried out in genomic DNA of the proband and parents with the terminal dideoxynucleotides method (*fmol* kit, Promega, Lyon, France). The forward primer was 5'CGAATATACAG AATGGATG, and the above-described oligonucleotide was the primer of the reverse strand. Manual sequencing reactions

were performed with ³²P-5'-primers labeled with [γ ³²P]ATP and polynucleotide kinase. Partially automated sequence analyses of both the sense and antisense strands extending to 30 to 40 bases of introns 5 and 6 were performed with 5'-labeled IRD800 primers according to the protocols of the SequiTherm kit (Epicentre Technologies, Madison, WI). Electrophoretic separation in acrylamide gels and analysis of the sequencing fragments were performed in a LI-COR DNA4000 sequencer with the software provided by the manufacturer (LI-COR Inc, Lincoln, Nebraska).

Results

T2-weighted MRIs demonstrated the presence of two cerebral cavernous malformations (CCMs) in the proband of the CV36 family. CCMs were not found in either parent (Fig 1) or the healthy sister (not shown) in a whole-brain screening.

The analysis of *CCM1* haplotypes showed that the siblings inherited the same chromosome from the father but different chromosomes from the mother (Fig 2). The haplotypes also revealed the lack of recombination in this region. Our first step in identifying the possible mutation was to obtain an illustrative SSCP in the PCR product of exon VI (see bands in Fig 2). A striking finding was that none of the progenitors shared the SSCP, suggesting a noninherited mutation in exon VI of *Krit1*.

Sequencing of the corresponding genomic regions included the sense and antisense strands of exon VI and at least 30 bases at the 3' end of intron 5 and 30 bases at the 5' end of intron 6. The sequencing of exon VI identified a 2-bp (TC/AG) deletion that is 48 bp from the splice junction with intron 6. The deletion of nucleotides 741T and 742C shifts the reading frame and predicts a mutated sequence of 23 amino acids (RNSAIFHYMGFFRKPQPSTQTIS) that ends with a TAA termination triplet. The 741delTC mutation substitutes the CAT triplet of histidine at position 271 with the stop codon (H271X). The sequencing of the sense and antisense strands clearly demonstrated the deletion in the genomic DNA of the proband and the normal sequence in parents. We did not find other mutations either in the coding region or in the boundary intronic sequences of exon VI of the proband or the relatives. Comparisons among the parents and proband of a set of polymorphic markers of independent loci excluded a possible false paternity or maternity ascription.

Discussion

The clinical symptoms of the index patient were compatible with a mutation of maternal origin because, in addition to antecedents of epilepsy in the grandfather, both the proband and her mother complained of headaches. The finding of two CCMs in the proband but not in relatives suggested a noninherited CCM. None-

theless, a familial form of CCM was not excluded by the aforementioned considerations, given the variable penetrance of this disease.

The proband did not inherit the disease allele from either parent, indicating that the patient represents a de novo mutation. This conclusion is supported by the following data: (1) the finding of the SSCP of exon VI in the patient but not in the parents or sister, (2) the demonstration of the 741delTC deletion in exon VI of the proband and the wild-type sequence in both parents and the healthy sister, (3) the demonstration of the deletion of the AG tandem in the antisense strand, (4) the absence of recombination in the interval of *CCMI*, and (4) the exclusion of a false maternity or paternity ascription.

The pathogenic mechanism of CCMs could be similar to the formation of the neurocutaneous tumor of tuberous sclerosis type 2 (*TSC2*), where tuberin, the product of the *TSC2* gene, functions as a tumor suppressor protein by acting as a GTPase activator for Krev-1/rap1a.⁹ The existence of either multiple or single lesions in hereditary and sporadic forms, respectively¹⁰ suggests the "Knudson double-loss mechanism" in cavernous angioma and evokes the hereditary and sporadic forms of retinoblastoma.⁵ The great variety of mutations described in the hereditary form of cavernous angioma²⁻⁴ suggest a high mutation rate of the *Krit1* gene. The results herein described are the first evidence of CCMs caused by a spontaneous mutation in the *Krit1* gene. Nonetheless, a sporadic cavernous malformation caused by a late or somatic mutation in a single cell in the nervous system can be excluded. In effect, such an event is not detectable in the genomic DNA extracted from peripheral leukocytes. The patient likely has a germline mutation, as evidenced by the deletion in peripheral leukocyte genomic DNA and the CCMs. Thus, this patient likely has a condition that is heritable by her offspring. In effect, the proband in this report represents a "founder" for a new lineage of individuals with familial cavernous malformation by virtue of a new mutation.

This study was supported by grant 99/0407 from Fondo de Investigaciones Sanitarias

References

1. Serebriiskii I, Estojak J, Sonoda G, et al. Association of Krev/rap1a with *Krit1*, a novel ankyrin repeat-containing protein encoded by a gene mapping to 7q21-22. *Oncogene* 1997;15:1043-1049.
2. Laberge-le Couteux S, Jung HH, Labauge P, et al. Truncating mutations in *CCMI*, encoding *Krit1*, cause hereditary cavernous angiomas. *Nat Genet* 1999;23:189-193.
3. Sahoo T, Johnson EW, Thomas JW, et al. Mutations in the gene encoding *Krit1*, a Krev-1/rap1a binding protein, cause cerebral cavernous malformations (*CCMI*). *Hum Mol Genet* 1999;8:2325-2333.
4. Zhang J, Clatterbuck RE, Rigamonti D, Dietz HC. Mutations

in *KRT1* in familial cerebral cavernous malformations. *Neurosurgery* 2000;4:1272-1276.

5. Knudson AG. Hereditary cancer: two hits revisited. *J Cancer Res Clin Oncol* 1996;122:135-140.
6. Jung HH, Labauge P, Laberge S, et al. Spanish families with cavernous angioma do not share the Hispano-American *CCMI* haplotype. *J Neurol Neurosurg Psychiatry* 1999;67:551-552.
7. Lucas M, Solano F, Zayas MD, et al. Spanish families with cerebral cavernous angioma do not bear the 742C→T Hispanic American mutation of the *KRIT1* gene. *Ann Neurol* 2000;47:836.
8. Sahoo T, Serebriiskii I, Kotova E, et al. Identification of the authentic full length amino acid sequence of *Krit1* (*CCMI*) utilizing a combination of computational gene-prediction tools and RT-PCR. *Am J Hum Genet* 2000;67(suppl 2):261.
9. Wienecker R, Konig A, DeClue JE. Identification of tuberin, the tuberous sclerosis-2 product: tuberin possesses specific Rap1GAP activity. *J Biol Chem* 1995;270:16409-16414.
10. Labauge P, Laberge S, Brunereau L, et al. Hereditary cerebral cavernous angiomas: clinical and genetic features in 57 French families. *Lancet* 1998;352:1892-1897

Abnormal Desmin Protein in Myofibrillar Myopathies Caused by Desmin Gene Mutations

Mian Li, MD, PhD, and Marinos C. Dalakas, MD

Muscle proteins were extracted in various sodium dodecyl sulfate buffers from 6 patients with myofibrillar myopathy (MFM) and previously identified with mutations in the desmin gene (desmin myopathy; DesM), 6 with MFM without mutations, and 14 disease controls to search for alterations in biochemistry and solubility of mutated desmin filaments. In the 1% posthigh-speed pellet fraction, desmin was detected with immunoblots only in DesM and not the other MFM. We conclude that mutant desmin forms insoluble aggregates that are specific for the DesM and can be detected with Western blots.

Ann Neurol 2001;49:533-536

From the Neuromuscular Diseases Section, National Institute of Neurological Diseases and Stroke, National Institute of Health, Bethesda, MD.

Received Jul 12, 2000, and in revised form Jan 9, 2001. Accepted for publication Jan 9, 2001.

Address correspondence to Dr Dalakas, Neuromuscular Diseases Section, NINDS, NIH, Building 10, Room 4N248, 10 Center Drive, MSC 1382, Bethesda, MD 20892-1382.
E-mail: dalakasM@ninds.nih.gov

Myofibrillar myopathies (MFM) are a heterogeneous group of inherited skeletal myopathies often associated with cardiomyopathies. Myofibrillar proteins, including desmin, actin, gelsolin, and dystrophin, accumulate in skeletal muscle fibers of biopsy specimens, but desmin is more consistently and abundantly found.¹⁻³ Desmin, a 53 kD type II intermediate filament protein, maintains the structural and functional integrity of the myofibrils and functions as a cytoskeletal protein linking individual myofibrils at the Z-band level to each other and to the sarcolemma. Mutations in the desmin gene cause a skeletal and cardiac myopathy, which is a distinct subset among the MFM group termed *desmin myopathy* (DesM).⁴⁻⁷ Because in DesM the deposits of desmin are histologically similar to those in the other MFM, it is fundamental to identify at the protein level whether in DesM the aggregated mutant desmin is different from the nonmutant desmin accumulated in the muscle fibers of other patients with MFM. Elucidating such differences may help us to understand the underlying disease mechanism and provide a screening tool for the diagnosis of DesM.

Patients and Methods

We studied desmin protein in muscle biopsy specimens from 6 patients with DesM caused by the recently reported desmin gene mutations⁴ and from 6 patients with other MFM without identifiable mutations in the desmin or α -B-crystalline gene. Desmin protein deposits on the muscle biopsies were prominent in both groups. For controls we studied muscles from patients with sporadic-inclusion-body myositis (3), Duchenne muscular dystrophy (2), unidentifiable muscular dystrophy (1), mitochondrial myopathy (2), vacuolar myopathy due to phosphofructokinase deficiency (2), paraneoplastic desmatomyositis (1), and human muscle with normal muscle morphology (3).

Fractionation of Proteins from Cell Extracts by Differential Centrifugation

Protein fractionation was based on the method of Coligan et al.⁸ In brief, six- μ -thick cryosections of muscle were centrifuged, washed in phosphate-buffered saline (pH 7.4), and resuspended in 20 μ l sodium dodecyl sulfate (SDS) lysis buffer of low concentration, 0.1% (w/v), or high concentration, 1% (w/v), containing 50 mM Tris-HCl (pH 7.5), 500 mM NaCl, 1% Nonidet P40, 0.5% sodium deoxycholate, 2 mM EGTA, 10% glycerol, 25 μ g/ml phenylmethylsulfonyl fluoride, 100 μ M leupeptin, and 10 μ g/ml aprotinin. The cell suspension was homogenized, incubated at 25°C for 5 hours, and centrifuged twice at low speed (600g) to remove nuclei, unbroken cell debris, and large insoluble particles. The supernatant containing solubilized proteins, such as desmin monomer, and partially solubilized proteins, such as tetramer aggregates, was collected as the postlow-speed supernatant fraction. To obtain an aggregate-enriched desmin protein and polymers fraction, a high-speed centrifugation at 100,000g for 90 minutes was performed.⁸ The pellet was

then resuspended in the sample buffer (NP0003; Novex, San Diego, CA) as the posthigh-speed pellet fraction.

Immunoblotting

Fifteen microliters of 20 μ g protein from either the postlow-speed supernatant fraction or the high-speed pellet fraction was prepared in 5 μ l sample buffer (NP0003; Novex) and incubated at 95°C for 5 minutes. The solubilized proteins were processed in 10% SDS-polyacrylamide gel, transferred onto a polyvinylidene difluoride membrane (Millipore, Bedford, MA), and probed with a mouse monoclonal IgG antibody against 1) desmin (catalog No. MDE II; Accurate Co., Westbury, NY) in 1:100 dilution, 2) α -tropomyosin of striated muscle (Accurate Co.) in 1:50 dilution, and 3) HSP27 (Chemicon International Inc., Temecula, CA) in 1:200 dilution. Antibody binding was detected with peroxidase-conjugated anti-mouse polyclonal IgG (Amersham International, Buckinghamshire, England). Enhanced chemiluminescence reagent (Amersham) was used to detect the immunoreactive bands. Antibody specificity for the striated muscle desmin was concurrently examined in extracts from skeletal muscle, cardiac muscle (Chemicon), and ovarian tumor containing smooth muscle. Some experiments were replicated using two additional mouse monoclonal antibody against desmin (clone DE-R-11; Novocastra Laboratories; and clone ZSD1; Zymed, Inc., San Francisco, CA).

Results

Desmin in the Postlow-Speed Supernatant Fraction (0.1% SDS)

As is shown in Figure 1A, the antidesmin antibody was specific for the desmin of the skeletal (see Fig 1, lanes 2, 3) and cardiac (see Fig 1, lane 4) muscle but not for the smooth muscle expressed in the tumor (see Fig 1, lane 1). Desmin migrated at a molecular weight of 57 kD, which is slightly higher than its predicted 53 kD. Specificity for striated muscle reactivity was internally controlled with reaction to α -tropomyosin (see Fig 1A, arrowhead, lanes 2-4).

Immunoblotting of proteins from postlow-speed supernatant fraction could not distinguish between the desmin of the normal or the disease control muscles and the desmin of MFM and DesM muscles, except for 2 patients (see Fig 1B). One of these patients had DesM with a 32-amino-acid deletion,⁴ corresponding to the lower molecular weight protein band (see Fig 1B, lane 7), which represents the mutant protein encoded by the mutant allele. The other patient (see Fig 1B, lane 9) had MFM but no detectable desmin gene abnormality.

Desmin in the Posthigh-Speed Pellet Fraction (0.1% SDS)

Immunoblotting of proteins in this fraction distinguished the desmin of MFM muscles from the others. As is shown in Figure 2, no reaction was noted in the normal control or the other muscle diseases (see Fig 2,

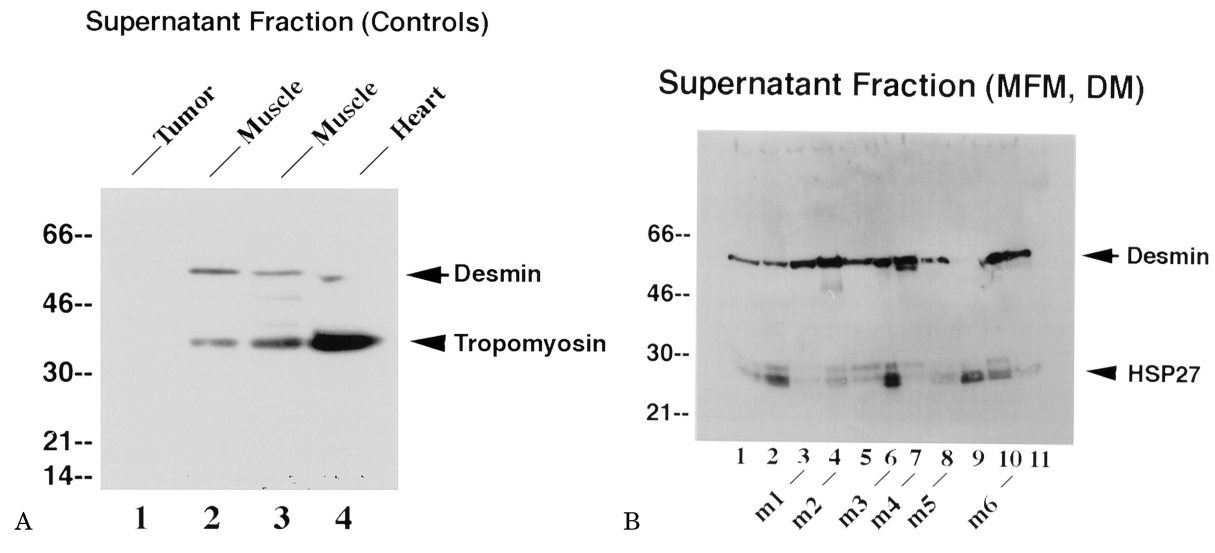


Fig 1. Western blot analysis of desmin of postlow-speed supernatant fraction prepared from control muscles (A) and myofibrillar myopathy (MFM; B). (A) Control specimens. Ovarian tumor tissue (lane 1) and muscle biopsy specimen (lane 2) from a patient with paraneoplastic dermatomyositis, muscle biopsy specimens from a patient with s-IBM (lane 3), and cardiac muscle from a normal human subject (lane 4). Monoclonal antibodies against desmin recognize a 57 kD protein (arrow) in striated muscles (lanes 2–4) but not the smooth muscle (lane 1). Monoclonal antibodies against α -tropomyosin of the striated muscle recognize a 35 kD protein (arrowhead, lanes 2–4), which was used as an internal control for loading the same amount of muscle protein. (B) MFM with desmin gene mutations (lanes 3, 4, 6–8, 10) or without identifiable mutations (lanes 1, 2, 5, 9, 11). In addition to the 57 kD protein (arrow), the monoclonal antibodies against desmin also recognize a protein with lower molecular weight in 1 patient (m4, lane 7) that correspond to the described deletion of 32 amino acids.⁴ As described elsewhere,⁴ the missense point mutations in m1 (lane 3) was in codon 337, changing the sequence from GCC to CCC; in m2 (lane 4) in codon 451, changing the ATC to ATG; in m3 and m5 (lanes 6, 8) in codon 360 and 393, resulting in G to C and A to T substitutions; and in m6 (lane 10) in codon 406, changing the sequence from CGG to TGG. No reactivity to desmin was seen in 1 patient (lane 9), although reactivity of HSP27 (arrowhead, lane 9) was present.

left, lanes 1–7). In contrast, strong immunoreactivity was noted in 5 of 6 DesM muscles (see Fig 2, left, lanes 8, 9, right lanes 3, 4, 6, 7, 10) and in 3 of 6 MFM muscles (see Fig 2, right, lanes 1, 5, 11). In spite of the marked differences in the desmin protein between the controls and the MFM muscles, the HSP27, which also forms aggregates during nonspecific stress, did not reveal differences between the two groups (see Fig 2, arrowhead).

Desmin in the Posthigh-Speed Pellet Fraction (1% SDS)

When the concentration of ionic detergent was increased to 1% SDS in the extraction buffer, immunoreactivity for desmin remained strong in the high-speed pellet fraction in 4 of 6 patients with DesM (Fig 3, lanes 3–5, 7) but in none of the other MFM without desmin gene mutations (see Fig 3, lanes 1, 8–11).

Discussion

We found that the mutant desmin intermediate filament protein exhibits altered biochemical properties and solubility, which are different from those of the wild-type

desmin protein. This finding offers an explanation for the formation of insoluble aggregates within the muscle fibers of DesM and provides a tool for confirming or detecting mutant desmin protein by Western blots in the majority (up to 66%) of patients with DesM.

In vitro, transient transfection assay revealed that mutant desmin proteins when introduced into fibroblasts do not form the normal intermediate filamentous network but become desmin aggregates.⁴ Although the normally insoluble desmin intermediate filament or polymer aggregates denature into soluble protein monomer with a strong detergent,⁹ the truncated intermediate filament proteins, such as desmin or keratin, remain in the insoluble fraction.^{10,11} In taking advantage of these biochemical alterations, the postlow-speed supernatant fraction, which consists of crude cell lysates, demonstrated no differences in the desmin protein between controls and the MFM or DesM muscles because mutations in 5 of the 6 DesM patients were in-frame point mutations that do not change the molecular weight of the protein. When differential centrifugation combined with increasing concentration of ionic detergent was used, clear biochemical differences

**Post-high speed (aggregate-enriched)
pellet fraction (0.1%SDS)**

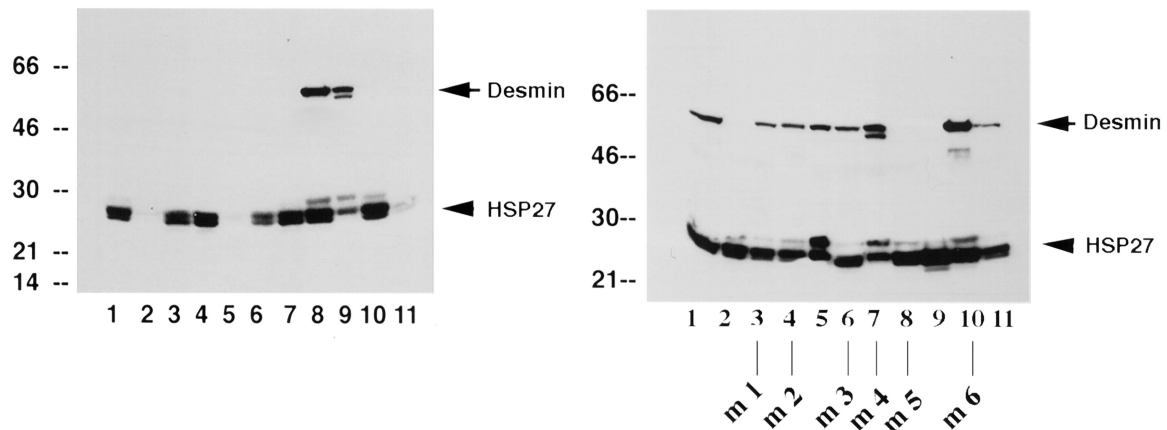


Fig 2. Western blot analysis of desmin of posthigh-speed pellet fraction (0.1% sodium dodecyl sulfate) from muscle biopsy specimens. Samples are from control patients (left, lanes 1–7) and 2 myofibrillar myopathy (MFM) patients with desmin gene mutations (lanes 8, 9). Samples from other MFM patients are shown at right (lanes 3, 4, 6–8, 10 for DesM and lanes 1, 2, 5, 9, 11 for MFM without mutations). Samples in lanes 8–10 in the left panel are the same as samples 10, 7, 2, respectively, in the right panel. (Left) No desmin reactivity was noted in non-MFM control muscles (lanes 1–7) compared to MFM with desmin gene mutations (lanes 8, 9). (Right) Strong desmin reactivity is evident (arrow) in 5 of the 6 specimens from MFM with desmin gene mutations and 3 of the 6 MFM without identifiable mutations.

were observed in the muscle protein extracts between MFM and controls (Fig 2). The distinction became more specific with 1% SDS, because under these conditions only the desmin from patients with DesM immunoreacted. Such immunoreactivity corresponds to the highly insoluble desmin aggregates we have observed not only in vitro within the muscle fibers of the DesM biopsies but also in the transfected cells in vitro,⁴ owing to the dominant negative effect of the mutant desmin protein.

During nonspecific cellular insults such as heat stress, HSP27 also forms aggregates and shows an early response for redistribution towards the insoluble fraction.^{12,13} Using HSP27 as an internal control, however, we demonstrated that the desmin protein abnormality is not a nonspecific phenomenon of protein aggregation within the muscle fibers but rather a primary insult underlying defects in the desmin protein as a consequence of desmin gene mutations. In contrast, in MFM with normal desmin gene, the desmin protein aggregates are secondary, resulting from primary defects in other unknown or known proteins connected with the intermediate filamentous network, such as α -B-crystallin.^{14,15}

Previous reports suggested a distinction between the desmin of MFM patients and normal controls on the basis of a 49 kD band reactivity in the desmin protein.^{16,17} In these studies, however, the degree of solu-

**Post-high speed (aggregated-enriched)
pellet fraction (1%SDS)**

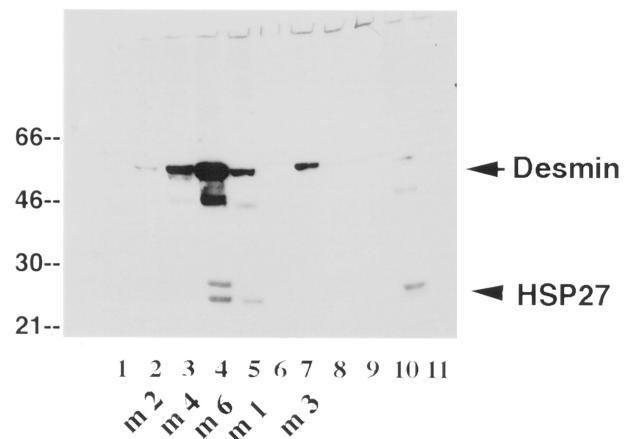


Fig 3. Western blot analysis of desmin of posthigh-speed pellet fraction (1% sodium dodecyl sulfate) from muscle biopsy specimens from myofibrillar myopathy (MFM) with desmin gene mutation (lanes 2–7) and MFM without identifiable gene mutations (lanes 1, 8–11). Strong desmin reactivity is noted in 4 of the 6 MFM with desmin gene mutations (lanes 3–5, 7) but not in the MFM without identifiable mutations.

bility was not considered, and correlation with desmin gene analysis was not performed to confer specificity for the altered desmin in patients with DesM.

In summary, enhanced desmin protein aggregates in the DesM muscle, as illustrated in this study, reflect the *in vivo* process of increased insoluble desmin protein, which cannot form normal filamentous network, owing to the desmin gene mutations. Although highly insoluble desmin appears to be specific for the DesM, desmin, which is more soluble than the mutated desmin but less soluble than the desmin in disease controls, also forms aggregates characteristic for MFM probably because of defects in other intermediate filament-associated proteins. Similar alterations in the protein solubility govern the disease pathogenesis in various neurodegenerative disorders in which aggregated proteins are formed within the targeted tissues.^{18–20}

Dr. Lev Goldfarb has identified our previously reported mutations in the studied patients (4,5).

References

1. Goebel HH. Desmin-related myopathies. *Curr Opin Neurol* 1997;10:426–429.
2. Nakano S, Engel AG, Akiguchi I, Kimura J. Myofibrillar myopathy. III. Abnormal expression of cyclin-dependent kinases and nuclear proteins. *J Neuropathol Exp Neurol* 1996;55:549–562.
3. Amato AA, Kagan-Hallett K, Jackson CE, et al. The wide spectrum of myofibrillar myopathy suggests a multifactorial etiology and pathogenesis. *Neurology* 1998;51:1646–1655.
4. Dalakas MC, Park K-Y, Semino-Mora C, et al. Desmin myopathy, a skeletal myopathy with cardiomyopathy caused by mutations in the desmin gene. *N Engl J Med* 2000;342:770–780.
5. Goldfarb LG, Park KY, Cervenakova L, et al. Missense mutations in desmin associated with familial cardiac and skeletal myopathy. *Nature Genet* 1998;19:402–403.
6. Munoz-Marmol AM, Strasser G, Isamat M, et al. A dysfunctional desmin mutation in a patient with severe generalized myopathy. *Proc Natl Acad Sci USA* 1998;95:11312–11317.
7. Sjoberg G, Saavedra-Matiz CA, Rosen DR, et al. A missense mutation in the desmin rod domain is associated with autosomal dominant distal myopathy, and exerts a dominant negative effect on filament formation. *Hum Mol Genet* 1999;8:2191–2198.
8. Coligan JE, Dunn BM, Ploegh HL, et al. Current protocols in protein science, vol 1. New York: John Wiley and Sons, Inc., 1997:6.1.6.
9. Darnell J, Lodish H, Baltimore D. Molecular cell biology, 2nd ed. Scientific American Books, Inc., 1990:894.
10. Raats JM, Gerards WL, Schreuder MI, et al. Biochemical and structural aspects of transiently and stably expressed mutant desmin in vimentin-free and vimentin-containing cells. *Eur J Cell Biol* 1992;58:108–127.
11. Coulombe PA, Hutton ME, Vassar R, Fuchs E. A function for keratins and a common thread among different types of epidermolysis bullosa simplex diseases. *J Cell Biol* 1991;115:1661–1674.
12. Caspers G-J, Bhat SP. The expanding small heat-shock protein family, and structure predictions of the conserved “ α -crystallin domain.” *J Mol Evol* 1995;40:238–248.
13. Suzuki A, Sugiyama Y, Hayashi Y, et al. MKBP, a novel member of the small heat shock protein family, binds and activates the myotonic dystrophy protein kinase. *J Cell Biol* 1998;140:1113–1124.
14. Vicart P, Caron A, Guicheney P, et al. A missense mutation in the alphaB-crystallin chaperone gene causes a desmin-related myopathy. *Nature Genet* 1998;20:92–95.
15. Engel AG. Myofibrillar myopathy. *Ann Neurol* 1999;46:681–683.
16. Arbustini E, Morbini P, Grasso M, et al. Restrictive cardiomyopathy, atrioventricular block and mild to subclinical myopathy in patients with desmin-immunoreactive material deposits. *J Am Coll Cardiol* 1998;31:645–653.
17. Lohrman JA, Janzer RC, Kuntzer T, et al. Familial cardiomyopathy and distal myopathy with abnormal desmin accumulation and migration. *Neuromuscul Disord* 1998;8:77–86.
18. Dobson CM. Protein misfolding, evolution and disease. *TIBS* 1999;24:329–332.
19. Lowe J, Blanchard A, Morrell K, et al. Ubiquitin is a common factor in intermediate filament inclusion bodies of diverse type in man, including those of Parkinson’s disease, Pick’s disease, and Alzheimer’s disease, as well as Rosenthal fibres in cerebellar astrocytomas, cytoplasmic bodies in muscles, and Mallory bodies in alcoholic liver disease. *J Pathol* 1988;155:9–15.
20. Hashimoto M, Takeda A, Hsu LJ, et al. Role of cytochrome c as a stimulator of α -synuclein aggregation in Lewy body disease. *J Biol Chem* 1999;274:28849–28852.

Effects of Riluzole on Cortical Excitability in Patients with Amyotrophic Lateral Sclerosis

Katja Stefan, MD, Erwin Kunesch, MD,
Reiner Benecke, MD, and Joseph Classen, MD

Using transcranial magnetic stimulation, the effect of riluzole (RLZ) on cortical excitability was studied in patients with amyotrophic lateral sclerosis (ALS). Paired-pulse inhibition (PPI) and paired-pulse facilitation (PPF) were reduced. RLZ partially restored deficient PPI in the first of 4 consecutive 3-month periods of testing, but left PPF unchanged. These findings substantiate the view that attenuation of glutamate-related excitotoxicity is an important factor contributing to the beneficial effect of RLZ in ALS.

Ann Neurol 2001;49:537–540

Riluzole (RLZ) modestly slows disease progression in amyotrophic lateral sclerosis (ALS) patients.^{1,2} RLZ has been shown to interact with glutamate-mediated neu-

From the Department of Neurology, University of Rostock, Germany
Received Sep 29, 2000 and in revised form Jan 18, 2001. Accepted for publication Jan 24, 2001.

Address correspondence to Dr Classen, Klinik für Neurologie und Poliklinik, Universität Rostock Gehlsheimer Str. 20, 18055 Rostock, Germany. E-mail: joseph.classen@med.uni-rostock.de

rotransmission at multiple pre- and postsynaptic sites.³ We used transcranial magnetic stimulation (TMS) to investigate serially the effects of RLZ on several parameters of cortical excitability in ALS patients.

Methods

The study was approved by the Ethics Committee of the University of Rostock and informed consent was obtained from all participants. Patients were included if they fulfilled the following criteria: 1. Clinical and EMG-evidence of ALS as defined by the El Escorial criteria;⁴ 2. TMS yielded a motor-evoked potential (MEP) of at least 0.5 mV in the extensor digitorum communis muscle (EDC); 3. The patients must be drug-naïve with respect to RLZ.

Twenty-two patients aged 35 to 81 years (64 ± 12 years; mean \pm SD) with ALS were screened for the study. Patients were treated with 100 mg RLZ daily.

Ten patients (51 ± 11 years) with pure upper (hereditary spastic paraplegia ($n = 2$) or lower motoneuron disorders (spinal muscular atrophy ($n = 3$), X-linked recessive bulbospinal neuronopathy ($n = 1$), multifocal motor neuropathy with conduction block ($n = 2$), pure motor neuropathies ($n = 2$) served as disease controls. Additionally, 13 age- and sex-matched healthy control subjects (52 ± 18 years) were tested.

Electromyogram (EMG) was recorded from the right extensor digitorum communis muscle. Raw signals were amplified, bandpass filtered between 20 and 2000 Hz, sampled at 5 kHz, and analyzed off-line.

Focal TMS was performed using a figure eight-shaped magnetic coil connected with a Magstim 200 magnetic stimulator (Magstim, Whitland, Dyfed, UK). For the paired-pulse experiments two stimulators were connected to the same coil through a BISTIM module (Magstim).

At the optimal position for eliciting a MEP in the resting right EDC the resting motor threshold (RMT) was determined as the stimulator intensity producing a response of at least 50 μ V in at least 5 of 10 consecutive trials.

Paired-pulse inhibition (PPI) and facilitation (PPF) were studied using a double-shock paradigm.⁵ Test stimulus intensity was adjusted to evoke an unconditioned MEP response with an amplitude of approximately 0.5 to 1.0 mV in the relaxed target muscle (TSI*). The intensity of the conditioning stimulus was set at 20% below RMT. Interstimulus intervals (ISIs) of 3 ms and 13 ms were selected, for PPI or PPF, respectively. EMG activity was monitored by visual and auditory feedback. The cortical silent period (SP) induced by TMS at 150% RMT was elicited while subjects held a tonic voluntary contraction of approximately 30% of their individual maximal force. Ten artifact-free trials were collected.

ALS patients were tested at the time of enrollment into the study and subsequently during treatment with RLZ. TMS testing under RLZ was done at least 5 days after initiation of RLZ therapy and in subsequent intervals of maximally 3-month duration over 1 year and as long as the patients were able and willing to return to the neurological department for outpatient visits and as long as an amplitude of at least 0.5 mV could be evoked in the relaxed EDC.

TMS-evoked MEP amplitudes were expressed as a fraction of the maximal muscle compound action potential elicited

by supramaximal electrical stimulation of the radial nerve (MEP%). The duration of the SP was determined as the time from stimulus onset to the time of reoccurrence of voluntary EMG activity.⁶ MEP amplitudes of mean conditioned responses (CR3 or CR13, for ISI of 3 ms and 13 ms, respectively) were expressed as percentage of the mean amplitude of the unconditioned test response. PPI and PPF are then given as (1) PPI = 100% - CR3, (2) PPF = CR13 - 100%. Results were compared between the ALS patients and the control groups employing unpaired two-tailed *t* tests. For time series, data from individual subjects were binned in 3-month intervals if more than one data point for a 3-month period was available for a subject.

Results

Of 22 ALS patients screened for the study, 9 patients did not meet the inclusion criteria because TMS failed to evoke an MEP in the resting EDC of sufficient size ($n = 7$), or the patients were already under RLZ when first seen ($n = 2$). The mean duration of symptoms at the time of the screening visit was 8.4 ± 5.9 months. Over the course of the study, all patients with initially suspected ALS eventually fulfilled the El Escorial criteria of definite ALS.

Results from all included ALS patients at baseline, matched healthy controls, and disease controls are presented in Table 1. CR3 was significantly increased in patients with ALS as compared to control groups, corresponding to a decrease of PPI (from a mean of 44.2% in controls to 3.1% in ALS patients). PPF was significantly reduced in ALS patients.

Of the 13 patients originally included, 3 were unavailable for retesting under RLZ therapy. In the remaining 10 ALS patients, baseline measurements of cortical excitability were compared to measurements obtained at least 5 days after initiating the RLZ therapy. Results are shown in Table 2. RLZ partially restored reduced PPI, on average, by 33.8%. In contrast to its effect on PPI, RLZ induced no change in PPF or the duration of the cortical silent period. TSI* and RMT under RLZ therapy were similar as before initiation of RLZ.

The increase of PPI associated with RLZ was present for only the first 3 months of therapy. Thereafter, PPI decreased again in 6 of 8 patients and returned to near the baseline levels (Fig a). PPF and duration of SP remained essentially unchanged during continuous therapy with RLZ.

PPI was within the normal range at the initial baseline assessment in 2 patients. In these patients PPI decreased after a 5- to 6-month follow-up. This decrease could partially be reversed by increasing the total daily dose from 100 to 150 mg RLZ (see Fig b).

Discussion

Because the principal mechanism of action of RLZ is well known,³ the effect of RLZ on distinct abnormal-

Table 1. Transcranial Magnetic Stimulation Parameters of Amyotrophic Lateral Sclerosis (ALS) Patients, Disease Controls, and Healthy Controls

Parameter	Healthy Controls	<i>p</i> value	ALS Patients	<i>p</i> value	Disease Controls
RMT (%)	40.1 ± 8.0	n.s.	37.7 ± 10.8	n.s.	43.3 ± 6.7
MEP (%)	55.1 ± 19.9	<i>p</i> < 0.05	39.6 ± 23.1	<i>p</i> < 0.02	61.2 ± 23.4
SP (ms)	152 ± 26	n.s.	146 ± 35	n.s.	159 ± 44
CR3 (%)	55.8 ± 15.3	<i>p</i> < 0.001	96.9 ± 35.9	<i>p</i> < 0.001	54.9 ± 14.6
CR13 (%)	155.1 ± 23.3	<i>p</i> < 0.002	128.7 ± 27.6	n.s.	152.8 ± 40.8

Data shown represents ± SD. *p* values refer to comparisons between ALS patients and healthy controls, and between ALS patients and disease controls, respectively.
n.s. = not significant.

ities in paired-pulse studies in ALS patients provides further insight into the pathogenesis of this disease as well as on the mechanisms by which RLZ may exert its beneficial effect in ALS.

Implications for the Pathogenesis of ALS

As other authors,⁷⁻¹² we have demonstrated an abnormal reduction of PPI in ALS patients. The impairment of PPI in ALS patients has been taken as evidence for a primary role of inhibitory interneurons in the pathogenesis of ALS,^{9,13} consistent with histopathological evidence of degradation of inhibitory interneurons.¹⁴ During the first 3 months of therapy, RLZ partially restored PPI in ALS patients, including full normalization in some. This finding would support a primary role of inhibitory interneurons only if RLZ were to exert a direct effect at inhibitory interneurons. However, RLZ does not directly interfere with γ -aminobutyric acid (GABA) release.¹⁵ Because the magnitude of PPI is also enhanced by antigitamatergic substances,^{16,17} the RLZ-induced increase of PPI in ALS patients likely is a consequence of its antigitamatergic property. By removal of excess glutamatergic excitation of PTCs or excitatory interneurons in the presence of RLZ, these neurons would again become sensitive to inhibitory GABAergic influences. Because inhibition could be fully normalized in some patients, a severe loss of inhibitory interneurons is unlikely and little effect on disease progression would be expected from attempts at restoring intracortical inhibition by GABAergic agents.

PPF was reduced in ALS patients in agreement with at least two previous studies.^{7,10} Furthermore, PPF remained unaffected by RLZ while PPI was substantially increased. The failure of RLZ to reduce PPF may reflect an insufficient reduction of glutamatergic stimulation of excitatory interneurons or of PTCs, implying that in unmedicated patients glutamatergic stimulation of these neurons, or their glutamate-mediated depolarization, would be grossly enhanced.

Findings by Ridding and colleagues¹⁸ may provide a complementary or alternative mechanism by which our results could be explained. These authors showed that PPI and PPF both decrease with voluntary activation.

Importantly, this phenomenon is generated cortically. It may thus be concluded that the neuronal elements mediating PPI and PPF are inhibited when pathways leading to PTC activity, or PTCs themselves, are active. The decrease of PPI and PPF in ALS could be explained by overactivity of the neuronal elements inhibiting the interneurons mediating PPI and PPF. RLZ may reduce the overactivity of these neuronal elements: PPI would then be increased and PPF would be enhanced. At the same time, an antigitamatergic effect of RLZ at the postsynaptic PTC membrane would decrease PPF, overall leaving PPF unchanged by RLZ in ALS patients.

Together, our results suggest that the decreases of PPI and PPF reflect either spontaneous or stimulation-induced overactivity at excitatory synapses. The origin of this overactivity may well include insufficient clearance of basal glutamate release from the synaptic cleft.¹⁹

Implications for the Mechanism of the Clinical Benefit Exerted by RLZ

Of several neurophysiological abnormalities in ALS patients, PPI was the only one that was partially normalized by RLZ. A significant effect of RLZ on PPI was observed exclusively during the first of 4 consecutive 3-month intervals of chronic drug therapy. Thus, the duration of the effect on PPI corresponded to the duration of the effect of RLZ on disease progression as

Table 2. Effect of Riluzole on Transcranial Magnetic Stimulation Parameters in Amyotrophic Lateral Sclerosis Patients

Parameter	-RLZ	+RLZ	<i>p</i> value
RMT (%)	35.7 ± 10.0	36.9 ± 12.2	n.s.
MEP (%)	44.5 ± 24.3	44.2 ± 26.8	n.s.
SP (ms)	149 ± 34	141 ± 31	n.s.
CR3 (%)	95.8 ± 41.4	62.0 ± 31.7	<i>p</i> < 0.05
CR13 (%)	131.3 ± 28.9	130.3 ± 27.4	n.s.

-RLZ = before riluzole therapy; +RLZ = measurement at 25 ± 24 days of continuous riluzole therapy.
n.s. = not significant.

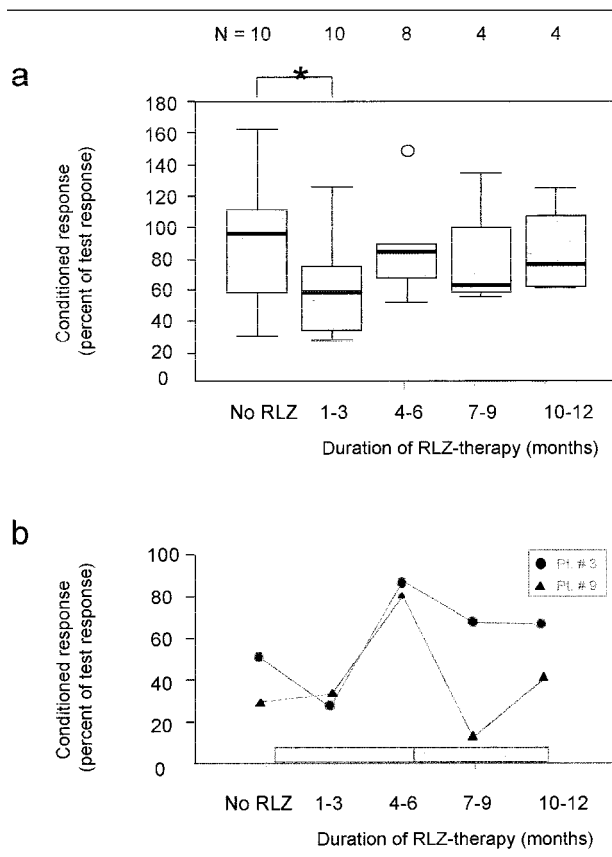


Fig. (a) Time course of effect of riluzole on paired-pulse inhibition (3 ms). Box plots of PPI in ALS patients before and at different 3-month intervals following initiation of RLZ therapy. Top row shows number of patients at different intervals. Asterisk indicates significant difference of PPI before and at 1- to 3-month interval (paired t test; $p < 0.05$). \circ = outlier at 4- to 6-month interval. (b) Partial reversal of delayed decrease of paired-pulse inhibition in 2 ALS patients by intensified riluzole-therapy. In two patients with initially normal PPI, CR3 increased between 5 and 6 months after initiating RLZ therapy equivalent to decrease of PPI. RLZ dosage was then increased from the standard dose of 100 mg (light gray) to 150 mg (dark gray). This resulted in a decrease of CR3 (partial renormalization of PPI).

known from clinical studies.^{1,2} This temporal congruency may suggest that the restoration of PPI is a neurophysiological marker of the beneficial clinical effect of RLZ and closely related to the underlying mechanism of this effect.

Future studies should address the question of whether RLZ therapy could be tailored to the needs of individual patients.

Supported by DFG Cl 95/3-1 and a grant-in-aid by Aventis (formerly Rhone-Poulenc Rorer), Germany.

References

- Bensimon G, Lacomblez L, Meininger V. A controlled trial of riluzole in amyotrophic lateral sclerosis. ALS/Riluzole Study Group. *N Engl J Med* 1994;330:585-591.
- Lacomblez L, Bensimon G, Leigh PN, et al. A confirmatory dose-ranging study of riluzole in ALS. ALS/Riluzole Study Group-II. *Neurology* 1996;47:S242-50.
- Doble A. The pharmacology and mechanism of action of riluzole. *Neurology* 1996;47:S233-S241.
- Brooks BR. El Escorial World Federation of Neurology criteria for the diagnosis of amyotrophic lateral sclerosis. Subcommittee on Motor Neuron Diseases/Amyotrophic Lateral Sclerosis of the World Federation of Neurology Research Group on Neuromuscular Diseases and the El Escorial "Clinical limits of amyotrophic lateral sclerosis" workshop contributors. *J Neurol Sci* 1994;124:96-107.
- Kujirai T, Caramia MD, Rothwell JC, et al. Corticocortical inhibition in human motor cortex. *J Physiol (Lond)* 1993;471:501-519.
- Triggs WJ, Macdonell RA, Cros D, et al. Motor inhibition and excitation are independent effects of magnetic cortical stimulation. *Ann Neurol* 1992;32:345-351.
- Hanajima R, Ugawa Y, Terao Y, et al. Ipsilateral corticocortical inhibition of the motor cortex in various neurological disorders. *J Neurol Sci* 1996;140:109-116.
- Yokota T, Yoshino A, Inaba A, Saito Y. Double cortical stimulation in amyotrophic lateral sclerosis. *J Neurol Neurosurg Psychiatry* 1996;61:596-600.
- Ziemann U, Winter M, Reimers CD, et al. Impaired motor cortex inhibition in patients with amyotrophic lateral sclerosis. Evidence from paired transcranial magnetic stimulation. *Neurology* 1997;49:1292-1298.
- Salerno A, Georgesco M. Double magnetic stimulation of the motor cortex in amyotrophic lateral sclerosis. *Electroencephalogr Clin Neurophysiol* 1998;107:133-139.
- Sommer M, Tergau F, Wischer S, et al. Riluzole does not have an acute effect on motor thresholds and the intracortical excitability in amyotrophic lateral sclerosis. *J Neurol* 1999;246:22-26.
- Caramia MD, Palmieri MG, Desiato MT, et al. Pharmacologic reversal of cortical hyperexcitability in patients with ALS. *Neurology* 2000;54:58-64.
- Enterzari-Taher M, Eisen A, Stewart H, Nakajima M. Abnormalities of cortical inhibitory neurons in amyotrophic lateral sclerosis. *Muscle Nerve* 1997;20:65-71.
- Nihei K, McKee AC, Kowall NW. Patterns of neuronal degeneration in the motor cortex of amyotrophic lateral sclerosis patients. *Acta Neuropathol (Berl)* 1993;86:55-64.
- MacIver MB, Amagasu SM, Mikulec AA, Monroe FA. Riluzole anesthesia: use-dependent block of presynaptic glutamate fibers. *Anesthesiology* 1996;85:626-634.
- Schwenkreis P, Liepert J, Tegenthoff M, Malin J-P. Influence of the glutamate antagonist riluzole on intracortical inhibitory and excitatory phenomena. *Electroencephalogr Clin Neurophysiol* 1997;103:54-16.
- Ziemann U, Chen R, Cohen LG, Hallett M. Dextromethorphan decreases the excitability of the human motor cortex. *Neurology* 1998;51:1320-1324.
- Ridding MC, Taylor JL, Rothwell JC. The effect of voluntary contraction on cortico-cortical inhibition in human motor cortex. *J Physiol (Lond)* 1995;487:541-548.
- Rothstein JD, Martin LJ, Kuncl RW. Decreased glutamate transport by the brain and spinal cord in amyotrophic lateral sclerosis. *N Engl J Med* 1992;326:1464-1468.

Gluten Sensitivity in Sporadic and Hereditary Cerebellar Ataxia

Khalafalla O. Bushara, MD,¹ Stephan U. Goebel, MD,³ Holly Shill, MD,¹ Lev G. Goldfarb, MD,² and Mark Hallett, MD¹

Gluten sensitivity, with or without classical celiac disease symptoms and intestinal pathology, has been suggested as a potentially treatable cause of sporadic cerebellar ataxia. Here, we investigated the prevalence of abnormally high serum immunoglobulin A (IgA) and IgG anti-gliadin antibody titers and typical human lymphocyte antigen (HLA) genotypes in 50 patients presenting with cerebellar ataxia who were tested for molecularly characterized hereditary ataxias. A high prevalence of gluten sensitivity was found in patients with sporadic (7/26; 27%) and autosomal dominant (9/24; 37%) ataxias, including patients with known ataxia genotypes indicating a hitherto unrecognized association between hereditary ataxias and gluten sensitivity. Further studies are needed to determine whether gluten sensitivity contributes to cerebellar degeneration in patients with hereditary cerebellar ataxia. Patients with hereditary ataxia (including asymptomatic patients with known ataxia genotype) should be considered for screening for gluten sensitivity and gluten-free diet trials.

Ann Neurol 2001;49:540–543

Celiac disease (CD) is an intestinal syndrome characterized by immunologic intolerance to wheat protein (gluten) leading to mucosal atrophy and malabsorption. CD has long been associated with progressive neurological deficits, predominantly cerebellar ataxia (with or without myoclonus) and peripheral neuropathy.^{2–4} Nervous system involvement in CD is believed to be the result of the disease rather than nutritional deficiencies related to malabsorption, such as vitamin E or vitamin B12 deficiencies.^{3,5} Earlier reports have mainly documented the occurrence of neurological deficits as complications of prediagnosed CD.^{2–4} However, more recent studies suggest that apparently

From the ¹Human Motor Control Section, and ²Clinical Neurogenetics Unit, National Institute of Neurological Disorders and Stroke; and ³Digestive Diseases Branch, National Institute of Diabetes, Digestive and Kidney Diseases, National Institutes of Health, Bethesda, MD.

Received Nov 2, 2000 and in revised form Jan 24, 2001. Accepted for publication Jan 24, 2001.

Address correspondence to Dr Mark Hallett, NIH, NINDS, Building 10, Room 5N226, 10 Center Drive MSC1428, Bethesda, MD 20892-1428. E-mail: hallettm@ninds.nih.gov

idiopathic cerebellar ataxia may be the presenting manifestation of gluten sensitivity.^{6–8} The diagnosis of gluten sensitivity, defined as “a state of heightened immunological responsiveness to ingested gluten in genetically predisposed individuals,” was made by demonstrating abnormally high titers of antibodies to gliadins (the major constituents of the gluten group of proteins)⁹ and supported by the presence of typical human lymphocyte antigen (HLA) class II genotypes (QD2, DR4 and QD8) known to be strongly associated with CD.¹⁰ Because the majority of patients with gluten sensitivity and ataxia lacked the classical CD symptoms or mucosal atrophy, it has been concluded that intestinal pathology is not a prerequisite for developing cerebellar degeneration, a situation similar to that of dermatitis herpetiformis where gluten sensitivity predominantly targets extraintestinal tissue.¹¹

The recognition of gluten sensitivity in patients with ataxia is important because it is potentially treatable and would also identify patients at risk for developing gastrointestinal malignancies reported in about 9% of untreated CD patients.¹² Previous reports of patients with ataxia and gluten sensitivity have implied a distinct type of disease, although the cerebellar syndrome described in these patients can be clinically indistinguishable from that of other ataxias including hereditary ataxias.⁸ In the current study, we investigated the prevalence of gluten sensitivity in a cohort of 50 patients with cerebellar ataxia, both sporadic and familial.

Materials and Methods

Patients were screened for IgG and IgA anti-gliadin antibodies (AGA) using enzyme-linked immunosorbent assay (ELISA) (SCIMEDX, Denville, NJ). We also measured anti-reticulin (ARA) and anti-endomysial (EmA) antibodies using indirect immunofluorescence (SCIMEDX) and anti-tissue transglutaminase (anti-tTG) antibodies using ELISA (Inova Diagnostics, Fairport, NY).¹³

Patients were tested for abnormal trinucleotide repeats expansion in genes of spinocerebellar ataxia (SCA) types 1, 2, 3, 6, 7, 8 and Friedreich's ataxia (FA). We also performed HLA typing, complete blood count, erythrocyte sedimentation rate, serum immunoglobulin assay (to exclude selective IgA deficiency), vitamin E, B12, folic acid, methylmalonic acid, plasma homocysteine, routine renal, liver, and thyroid function tests, rheumatoid factor, Sjögren syndrome, and antinuclear, thyroid, and paraneoplastic antibodies (Anti Hu, Ri, and Yo) tests. All patients had brain magnetic resonance imaging (MRI) performed and, when clinically indicated, underwent electromyography and nerve conduction studies (EMG/NCS). Upper gastrointestinal endoscopy and duodenal biopsy were performed in patients with positive anti-gliadin antibodies (see Results).

Results

Twenty-six patients had sporadic disease with no family history of ataxia and negative genetic tests (Table

Table 1. Patients with Sporadic Cerebellar Ataxia

Patient's number	Age	Sex	Duration (years)	GI	Ataxia: gait/limb/eye/speech	Other findings	AGA: IgA/IgG	HLA	Other lab
1	53	M	2	-	+ / + / + / 0	Myoclonus, extensor plantars	- / -	-	+RF
2	79	M	2	-	+ / + / 0 / 0	-	- / -	-	-
3	74	F	5	-	+ / + / + / +	Brisk reflexes, restless legs	- / -	-	-
4	75	M	10	-	+ / 0 / + / 0	-	- / -	DQ2, DR4	+RF
5	31	F	4	-	+ / + / 0 / 0	ADN	- / -	DQ2	IDDM
6	62	F	10	-	+ / + / + / +	-	- / -	-	-
7	63	F	2	-	+ / + / + / +	-	- / -	-	-
8	67	F	6	-	+ / + / 0 / 0	-	- / -	-	-
9	68	F	11	+	+ / + / + / +	Extensor plantars	- / -	-	-
10	55	F	20	+	+ / + / + / 0	Brisk reflexes, myoclonus	- / -	DQ2-DR4	-
11	18	M	8	-	+ / + / 0 / 0	Spasticity, brisk reflexes	- / -	N/A	Thrombocytopenia
12	62	F	5	-	+ / + / + / 0	Extensor plantars	- / -	-	Temporal meningioma
13	70	M	3	-	+ / 0 / + / 0	ADN	- / -	-	-
14	13	F	3	+	+ / + / + / +	Optic atrophy, extensor plantars	- / -	-	-
15	62	M	20	-	+ / + / + / +	Extensor plantars, ADN	- / -	-	-
16	64	F	12	-	+ / + / + / 0	-	- / -	-	-
17	28	F	9	-	+ / + / + / +	Ophthalmoplegia	- / -	DQ2	High ESR
18	53	M	5	-	+ / + / + / +	-	- / -	-	-
19	31	F	2	-	+ / + / + / +	-	- / -	DQ2	-
20	71	M	5	-	+ / + / + / +	-	+ / +, R, T	-	Anemia, high ESR
21	51	M	4	-	+ / + / + / 0	-	- / +	DQ2	High ESR
22	55	F	4	-	+ / 0 / + / 0	-	+ / -	DQ2	-
23	62	M	8	-	+ / + / + / +	Hypertonia, extensor plantars	+ / +, R	DR4	-
24	50	M	3	-	+ / + / + / +	-	+ / -, R	-	-
25	64	F	10	-	+ / + / 0 / 0	Cervical dystonia, AN	+ / -	DQ2	-
26	49	M	4	-	+ / + / + / 0	-	- / +	DQ2	-

GI = gastrointestinal symptoms; gait = gait ataxia; limb = limb ataxia; eye = nystagmus, dymeric, or slow saccades; speech = dysarthria; + = present; 0 = absent; Other findings = abnormal findings on clinical examination or electromyography/nerve conduction study; AN = axonal neuropathy; ADN = axonal/demyelinating neuropathy; AGA = anti-gliadin antibodies; R = positive anti-reticulins; T = positive anti-tissue-transglutaminase antibodies; Other lab = abnormal laboratory findings; RF = rheumatoid factor; ESR = erythrocyte sedimentation rate; IDDM = insulin-dependent diabetes.

1). Twenty-four patients (of 24 different families) had a known ataxia gene defect and/or family history suggestive of an autosomal-dominant inheritance pattern (Table 2). Seven of 26 patients with sporadic ataxia (27%) and 9 of 24 patients with hereditary ataxia (37%) had positive IgG, IgA, or both AGA (IgG or IgA-AGA levels > 25 U/mL). None had EmA-IgA antibodies. Three patients had anti-tTG antibodies (1 with sporadic and 2 with hereditary ataxia) and were also positive for AGA and ARA (patients 20, 49, and 50; see Tables 1 and 2). Intestinal biopsy (obtained in 15 of 16 patients with positive AGA) showed normal duodenal mucosa (8 patients) or inflammatory changes with lymphoplasmocellular infiltration and focal villous blunting but no crypt hyperplasia (patients 20, 23, 24, 25, 45, 49, and 50). There was no apparent difference in gastrointestinal symptoms, age of ataxia onset, incidence of peripheral neuropathy, myoclonus, or other neurological findings between AGA-positive and AGA-negative or between hereditary and sporadic ataxia groups (see Tables 1 and 2). HLA type DQ2 or DR4/DQ8 was present in 85% and 88% of AGA positive compared to 28% and 46% of AGA negative sporadic and hereditary ataxia, respectively. Except for the abnormalities shown in Tables 1 and 2, hematological, biochemical, and autoimmune profiles were normal. In all patients, cerebellar atrophy (with or without brain

stem or global brain atrophy) was evident on brain MRI.

Discussion

In agreement with previous studies, our results indicate a high prevalence of gluten sensitivity (as indicated by positive AGA) in patients with cerebellar ataxia (16/50; 32%). Also consistent with previous studies, we found that symptoms of malabsorption, villous atrophy, EmA-IgA, and anti-tTG antibodies are absent in the majority of AGA-positive patients. EmA-IgA were shown to be specific for severe mucosal disease and their absence is consistent with a predominantly extraintestinal pathology.¹⁴

The new and unexpected finding of the current study is that the prevalence of gluten sensitivity was similarly high in both sporadic and hereditary ataxias including those with identified gene defects. This indicates a previously unrecognized association between gluten sensitivity and autosomal dominant ataxias. In contrast to our findings, Pellecchia and colleagues found negative AGA in 23 patients with hereditary ataxia (6 with SCA2 and 17 with FA).⁸ Although the reason for this discrepancy is currently unclear, it is unlikely to be attributed entirely to the difference in hereditary ataxia types studied, as all of our SCA2 pa-

Table 2. Patients with Hereditary Cerebellar Ataxia

Patient's number	Age	Sex	Duration (years)	FH	Ataxia: gait/ limb/eye/ speech	Other findings	Genetics	AGA: IgA/ IgG	HLA	Other lab
27	16	F	2	+	+/+/+/+	—	SCA1	-/-	—	—
28	39	F	9	+	+/+/+/+	—	SCA3	-/-	—	—
39	62	M	12	+	+/+/+/0	—	SCA3	-/-	DR4	Low B12
30	34	F	10	+	+/+/0/0	—	SCA3	-/-	—	—
31	43	F	3	+	+/+/+/+	Extensor plantars	SCA3	-/-	—	+ RF
32	27	F	9	-	+/+/+/0	Extensor plantars	SCA3	-/-	DR4	Low vitamin E
33	31	F	6	+	+/+/0/0	—	SCA5*	-/-	—	—
34	71	F	9	+	+/+/0/0	—	SCA6	-/-	DR4	—
35	61	F	3	+	+/+/0/+	—	SCA6	-/-	—	—
36	62	M	5	+	+/+/+/+	—	SCA6	-/-	DQ2	—
37	27	M	3	+	+/+/+/+	—	AD	-/-	DQ2	—
38	31	F	15	-	+/+/0/0	—	AD	-/-	—	—
39	43	M	13	+	+/+/+/0	—	AD	-/-	DQ2	—
40	29	F	7	-	+/+/+/0	Extensor	FA	-/-	DQ2	—
41	20	F	4	-	+/+/+/0	Extensor plantars	FA	-/-	—	High ESR
42	32	F	12	+	+/+/+/0	—	AD	-/+	DR4	—
43	48	M	10	+	+/+/+/0	Ophthalmoplegia	SCA2	+/-	DQ2	—
44	37	F	11	+	+/+/+/+	Extensor plantars	SCA2	+/-	DQ2	—
45	39	M	7	+	+/+/+/+	Ophthalmoplegia	SCA2	+/-	DQ2	—
46	30	M	10	-	+/+/+/+	—	SCA2	+/-	DR4	—
47	65	F	20	+	+/+/+/0	—	SCA2	+/-	DQ2	—
48	64	F	13	+	+/+/0/+	—	SCA3	+/-	DQ2	Anemia, high
49	63	F	5	+	+/0/0/0	—	SCA8	+/-R,T	DR4-DQ8	High ESR
50	43	F	10	+	+/+/0/0	ADN	AD	+/+,R,T	—	Low vitamin E

*Member of the family reported in 17.

FH = family history of ataxia; Gait = gait ataxia; limb = limb ataxia; eye = nystagmus, dyometric, or slow saccades; speech = dysarthria; + = present; 0 = absent; Other findings = abnormal findings on clinical examination or electromyography/nerve conduction study; ADN = axonal/demyelinating neuropathy; AD = autosomal dominant; AGA = anti-gliadin antibodies; R = positive anti-reticulin; T = positive anti-tissue-transglutaminase antibodies; Other lab = abnormal laboratory findings; RF = rheumatoid factor; ESR = erythrocyte sedimentation rate.

tients (5 patients belonging to 5 different families) were AGA positive.

Evidence from clinical and pathological studies in celiac disease suggests a causal relationship between gluten sensitivity and cerebellar degeneration.²⁻⁴ Purkinje cell loss has been the most consistently reported neuropathological finding in celiac disease.¹⁵ Antibodies to gliadin have been found in the cerebrospinal fluid of gluten-sensitive patients with cerebellar ataxia and myoclonus (Ramsay Hunt syndrome)¹⁶ and recently, Hadjivassiliou reported lymphocytic cerebellar infiltration suggesting an immune-mediated direct insult to the nervous system.⁷ In support of this view is the improvement of ataxia documented in some patients treated with a gluten-free diet, indicating the potential reversibility of cerebellar dysfunction.^{7,17} On the other hand, the majority of patients reported showed no appreciable clinical response to a gluten-free diet. Although the reason for this is unclear, it has been attributed to factors such as dietary noncompliance (especially in patients with no gastrointestinal symptoms) or the irreversibility of neural damage resulting from long disease duration prior to treatment.^{6,7}

The lack of response to dietary restrictions in previous reports and our finding in patients with hereditary ataxia a high frequency of positive AGA may indicate the irrelevance of gluten sensitivity to the cerebellar de-

generation or that positive AGA is the consequence of cerebellar degeneration caused by other factors. However, one possibility is that gluten sensitivity may contribute to the degenerative process in hereditary ataxias. Further studies are needed to clarify this important issue given the lack of effective treatment for hereditary ataxia. Patients with hereditary cerebellar ataxia (including asymptomatic patients with known ataxia gene defect) should be considered for screening for gluten sensitivity and trials of gluten-free diet to determine whether dietary intervention improves ataxia, slows its progress, or delays its onset in those with gluten sensitivity.

References

1. Marsh MN. The natural history of gluten sensitivity: defining, refining and re-defining. *Q J Med* 1995;88:9-13.
2. Cooke WT, Smith WT. Neurological disorders associated with adult coeliac disease. *Brain* 1966;89:683-722.
3. Muller AF, Donnelly MT, Smith CM, et al. Neurological complications of celiac disease: a rare but continuing problem. *Am J Gastroenterol* 1996;91:1430-1435.
4. Bhatia KP, Brown P, Gregory R, et al. Progressive myoclonic ataxia associated with coeliac disease. The myoclonus is of cortical origin, but the pathology is in the cerebellum. *Brain* 1995; 118:1087-1093.
5. Ward ME, Murphy JT, Greenberg GR. Celiac disease and spinocerebellar degeneration with normal vitamin E status. *Neurology* 1985;35:1199-1201.

6. Hadjivassiliou M, Gibson A, Davies JG, et al. Does cryptic gluten sensitivity play a part in neurological illness? *Lancet* 1996;347:369–371.
7. Hadjivassiliou M, Grunewald RA, Chattopadhyay AK, et al. Clinical, radiological, neurophysiological, and neuropathological characteristics of gluten ataxia. *Lancet* 1998;352:1582–1585.
8. Pellecchia MT, Scala R, Filla A, et al. Idiopathic cerebellar ataxia associated with celiac disease: lack of distinctive neurological features. *J Neurol Neurosurg Psychiatry* 1999;66:32–35.
9. Wieser H. The precipitating factor in coeliac disease. *Baillieres Clin Gastroenterol* 1995;9:191–207.
10. Kaknoff MF. Genetic basis of coeliac disease—role of HLA genes. In: Marsh MN, ed. *Coeliac disease*. Boston: Blackwell, 1992:215–238.
11. Hadjivassiliou M, Grunewald RA, Davies-Jones GA. Gluten sensitivity: a many headed hydra. *BMJ* 1999;318:1710–1711.
12. Cooper BT, Holmes GK, Ferguson R, Cooke WT. Celiac disease and malignancy. *Medicine (Baltimore)* 1980;59:249–261.
13. Dieterich W, Ehnis T, Bauer M, et al. Identification of tissue transglutaminase as the autoantigen of celiac disease. *Nat Med* 1997;3:797–801.
14. Volta U, Molinaro N, De Franchis R, et al. Correlation between IgA anti-endomysial antibodies and subtotal villous atrophy in dermatitis herpetiformis. *J Clin Gastroenterol* 1992;14:298–301.
15. Kinney HC, Burger PC, Hurwitz BJ, et al. Degeneration of the central nervous system associated with celiac disease. *J Neurol Sci* 1982;53:9–22.
16. Chinnery PF, Reading PJ, Milne D, et al. CSF antigliadin antibodies and the Ramsay Hunt syndrome. *Neurology* 1997;49:1131–1133.
17. Collin P, Pirttila T, Nurmikko T, et al. Celiac disease, brain atrophy, and dementia. *Neurology* 1991;41:372–375.